Neutron Detectors

Sven C. Vogel

Materials Science & Technology Division &
Los Alamos Neutron Science Center

Los Alamos National Laboratory
Los Alamos, New Mexico, USA

LA-UR-24-23417

Somewhat last minute presentations, therefore:

Neutron Detectors Sven has worked with and can say something about

Sven C. Vogel

Materials Science & Technology Division &
Los Alamos Neutron Science Center

Los Alamos National Laboratory
Los Alamos, New Mexico, USA

LA-UR-24-23417

General principles

- Neutrons do not like to interact with materials in general
- Neutron interaction is generally
  - Isotope-dependent
  - Neutron energy dependent (the lower the energy, the more likely will the interaction happens)
  - Reducing neutron energy by moderation can make detection more likely
  - Shielding a neutron detector with e.g. cadmium can "reject" lower energy thermal neutrons to detect only epithermal neutrons
- Some "special" materials can detect neutrons
- Need electric signal to detect something electronically
- Some detectors like bubble chambers do NOT produce electric signals
- Neutron detector materials are highly absorbing and can typically also be used for shielding or collimation
- Focus on neutron detectors for scientific applications, for health physics/radiation protection applications see e.g. https://www.nrc.gov/docs/ML1122/ML11229A713.pdf

Characteristics of Neutron Detectors

- Interaction of the neutron with the detector material
- Half-life of the nuclear reaction
- Emission time of photons resulting from γ and neutron capture (discrimination)
- Dead time (while photons from a capture event are emitted, the detector is blind)
- Gamma sensitivity (neutrons rarely occur without gammas)
- Sensitivity/efficiency
  - Generally varies as a function of neutron energy, need to know neutron energy
  - Can be used to “filter” neutron fluxes
- Measurement of dose rate (total intensity) vs. time-of-flight (intensity as a function of time)
- Operational requirements:
  - High voltage
  - Vacuum
  - Toxic materials (e.g. BF_3 gas counters)
  - Radioactive materials (e.g. uranium fission chambers)

Interactions allowing to detect neutrons: Prompt reactions

- Absorption $\Rightarrow$ leads to activated nucleus $\Rightarrow$ leads to decay
  - Need large probability of neutron capture ("absorption") otherwise efficiency is too low (neutrons just pass through)
  - "Prompt" decay: "short" half-life of the activated state
  - What "short" means depends on the application:
    - For thermal (meV) neutrons, flight-path length is from 1-100 m $\Rightarrow$ time-of-flight is on the order of milliseconds, therefore ~1 microsecond might be acceptable depending on flux an resulting dead time
    - For fast (MeV) neutrons, with the same L, time-of-flight is on the order of microseconds $\Rightarrow$ prompt is <10 ns
  - Examples are helium-3, lithium-6, boron-10, uranium-235, gadolinium

Interactions allowing to detect neutrons: Reactions with longer half-lives

- Absorption $\Rightarrow$ leads to activated nucleus $\Rightarrow$ leads to decay
  - Need large probability of neutron capture (“absorption”) otherwise efficiency is too low (neutrons just pass through)
  - “Slow” decay: “longer” half-life of the activated state
  - What “longer” means depends on the application:
    - Radiation monitoring (half life spreads out high instantaneous flux)
      $\Rightarrow$ half-life needs to be short enough to alarm within seconds
    - Absolute flux measurement
      $\Rightarrow$ half-life needs to be long enough to walk from beam line to counter,
      $\Rightarrow$ short enough to be done counting within minutes or hours
  - Examples are gold, silver

Interactions allowing to detect neutrons: Proton recoil

- Scattering or "proton recoil"
- MeV neutron knocks out atoms in the detector
- Knocked out atoms create ions
- The more energy is transferred, the more likely/easy to detect
- Most energy is transferred when mass of knocked out atoms is ~mass of neutron $\Rightarrow$ hydrogen atoms $\Rightarrow$ "proton recoil"
- Examples are plastic scintillators (EJ200), organic glasses

Scintillators

- Scintillator: Material that exhibits luminescence (emits light) when excited by ionizing radiation
  $\Rightarrow$ for detection material needs to be transparent for visible light
  $\Rightarrow$ either clear glass, clear liquid, clear plastic, or clear single crystals
  $\Rightarrow$ grain boundaries in polycrystalline material stop light
- Light generation can be achieved by nuclear reaction (<1 keV neutrons) or proton recoil (>0.5 MeV)
- Nuclear reaction must have "short" half-life (depends on event rates, applications etc.)
- Light is typically amplified by photo-multiplier tube (PMT) and converted to electrical signal
- Emitted light pulse for neutron or gamma is ideally different
  $\Rightarrow$ pulse shape discrimination (PSD)
- Alternatively, light can be viewed by camera for radiography
- If too many events, setup can be used in current mode (no individual events, no dead time)

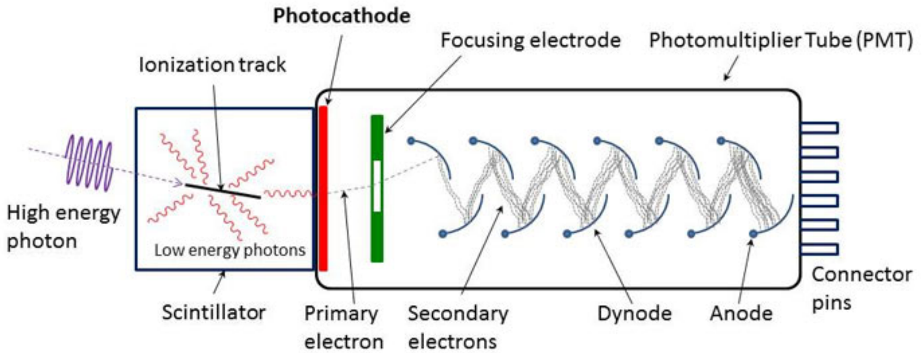

https://academy.berkeleynucleonics.com/courses/655995/lectures/11699530

Scintillators: Pulse shape discrimination

- Example: LiF:ZnS(Ag)
  ⇒ Mixture of Li-6 enriched lithium fluoride and zinc sulfide doped with silver
  ⇒ Used for neutrons <100 eV
- Digitized photomultiplier output provides electric signal for
  - Gammas (high pulse, <300 ns short)
  - Neutrons (lower pulse, >300 ns)
  - Noise (lower pulse, <200 ns)
- Signals allow to discriminate gammas from neutrons
- Parameters depend on the scintillator material
- Art is to create materials that make discrimination easy, have low noise, allow to do this in short time (avoid dead time) etc. (life is full of compromises)

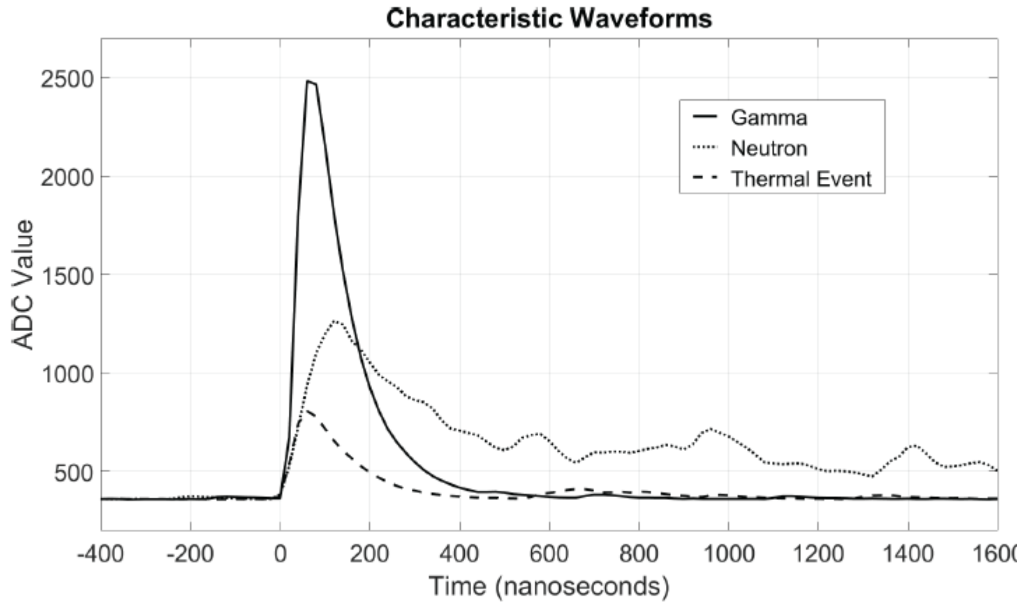

Fig. 3. Example waveforms for neutrons, gammas, and thermal noise.

Pritchard et al, IEEE Transactions on Nuclear Science **67** (2020) 414

Scintillators: Pulse shape discrimination

- Example of pulse shape discrimination for LiF:ZnS(Ag):
  - Integrate measured voltage for region W1 typical for gamma event duration
  - Integrate second region W2 after region W1 for longer period
  - Record events for a pure gamma source (Cs-137)
  - Record events for a neutron source (has also gammas)
  - Plot integrated values for W2 vs. W1
- Optimize integration windows, find thresholds etc
- Problem: No radiography with photomultipliers, dead time can become an issue (detector saturation)

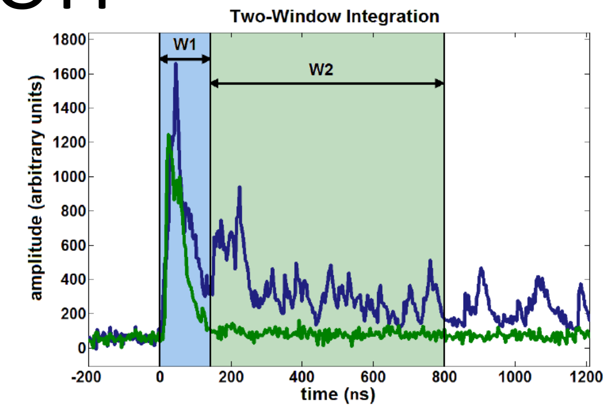

Fig. 5. This is a diagram of the two-window CC algorithm. The green

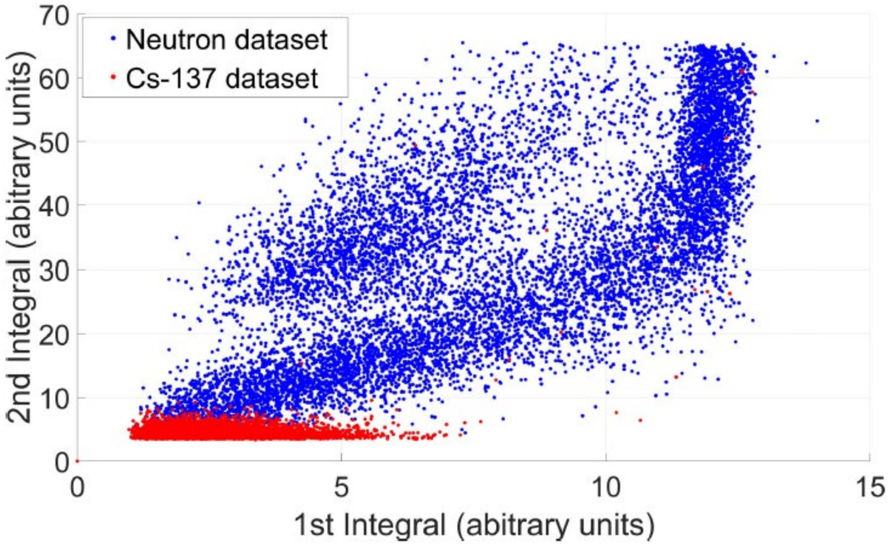

Fig. 6. Scatter plot of the neutron and gamma data sets using the two-window CC algorithm. Preamplifier saturation "chops off" the peaks of large neutron waveforms. This distortion is seen in the scatter plot as the first integral approaches a value of 12. Saturation at high energy does not affect neutron ID.

Pritchard et al, IEEE Transactions on Nuclear Science **67** (2020) 414

What makes a good neutron detector?

- Besides getting light out, a good neutron detector has a high probability to interact with a neutron…
- Absorption cross-section!
- Good source for cross-sections:
  Table of Nuclides at Korea Atomic Energy Research Institute (https://atom.kaeri.re.kr/nuchart/)

Obtaining cross-sections: Open https://atom.kaeri.re.kr/nuchart/

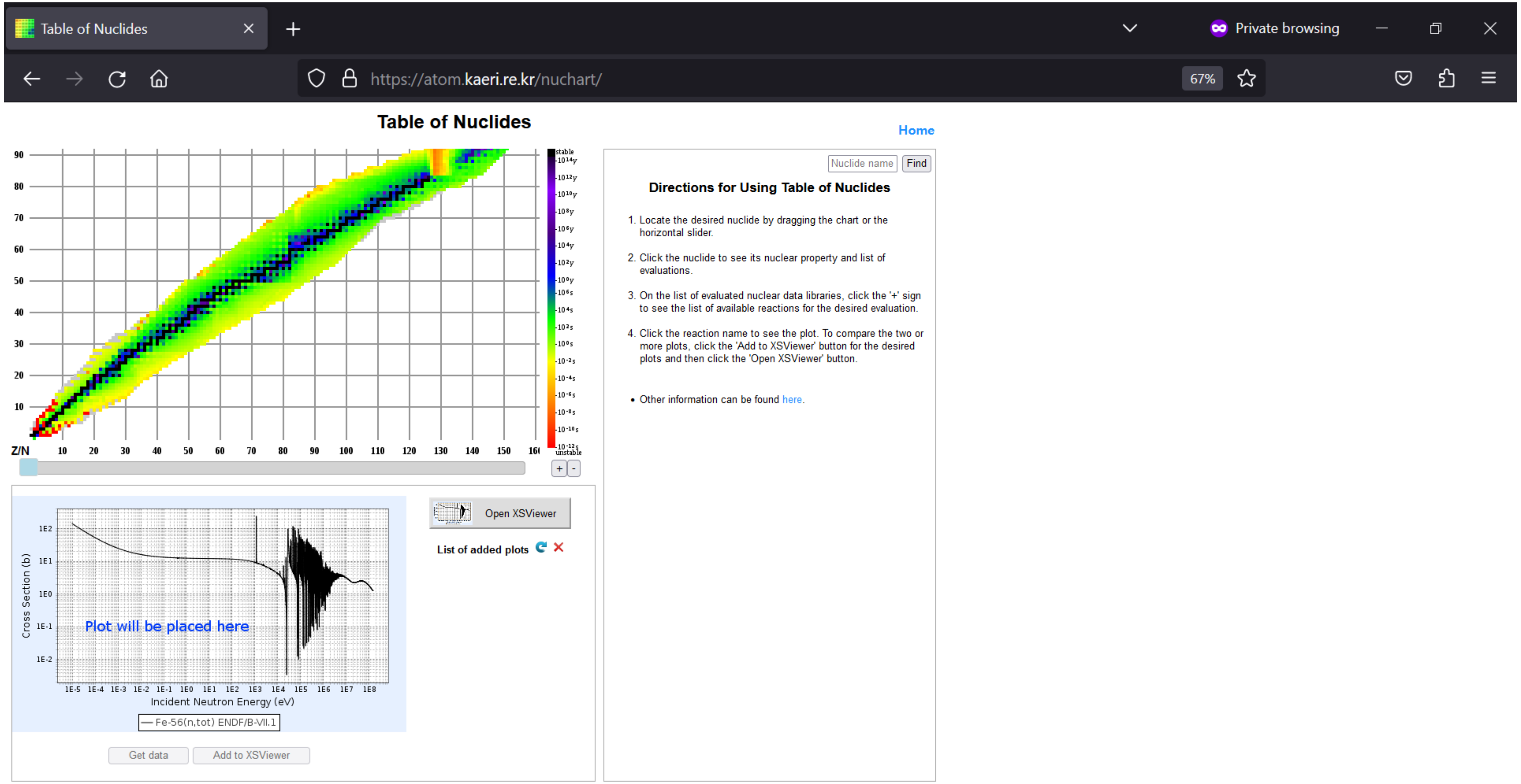

Obtaining cross-sections
Search for boron ⇒ “B”, find stable isotopes

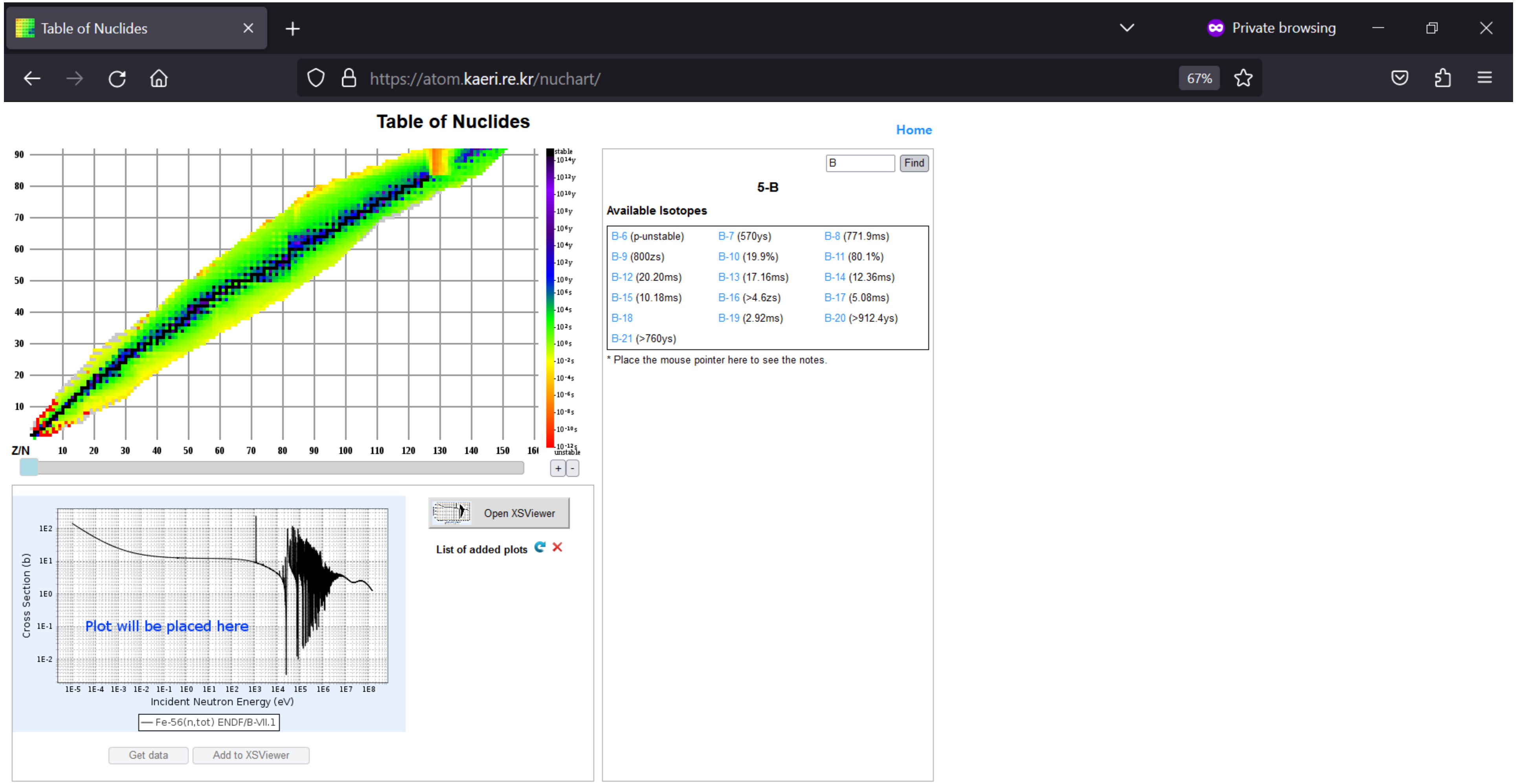

Obtaining cross-sections
Select B-10, open ENDF record, click "plot", click "Add to XSViewer"

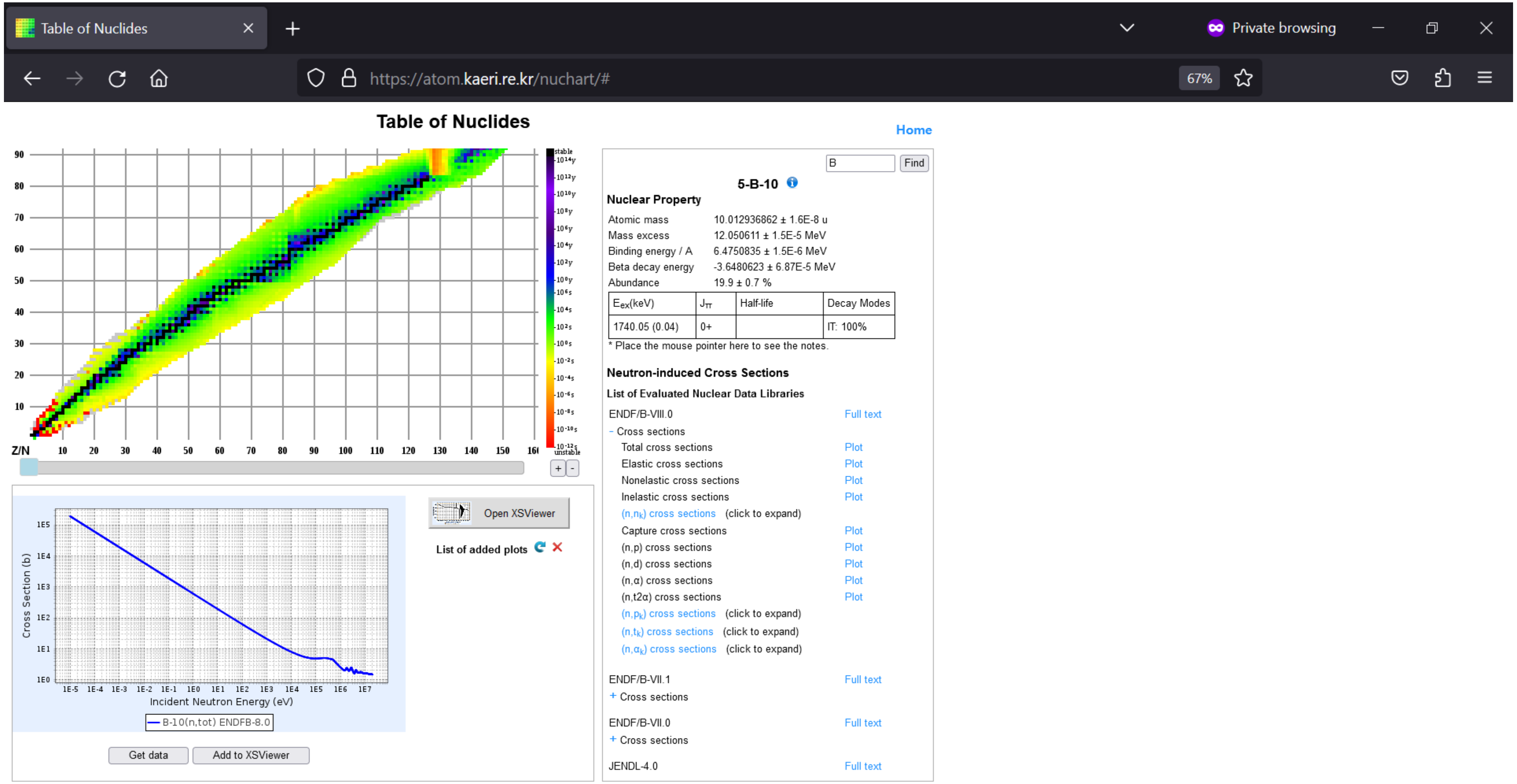

Obtaining cross-sections
Select B-11, open ENDF record, click “plot”, click “Add to XSViewer”, click “Open XSViewer”

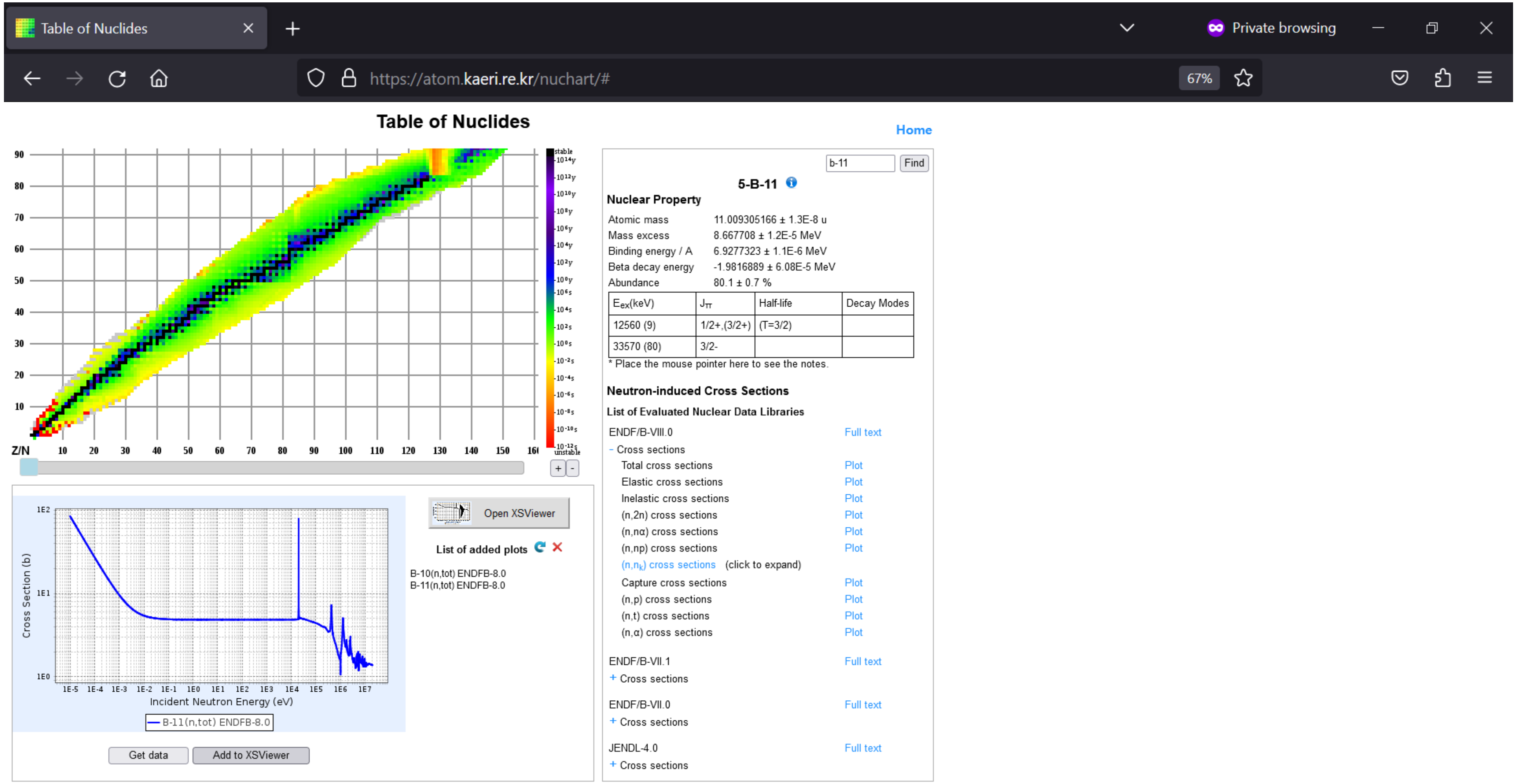

Cross-sections for B-10 & B-11 compared
⇒To study borides you want B-11!

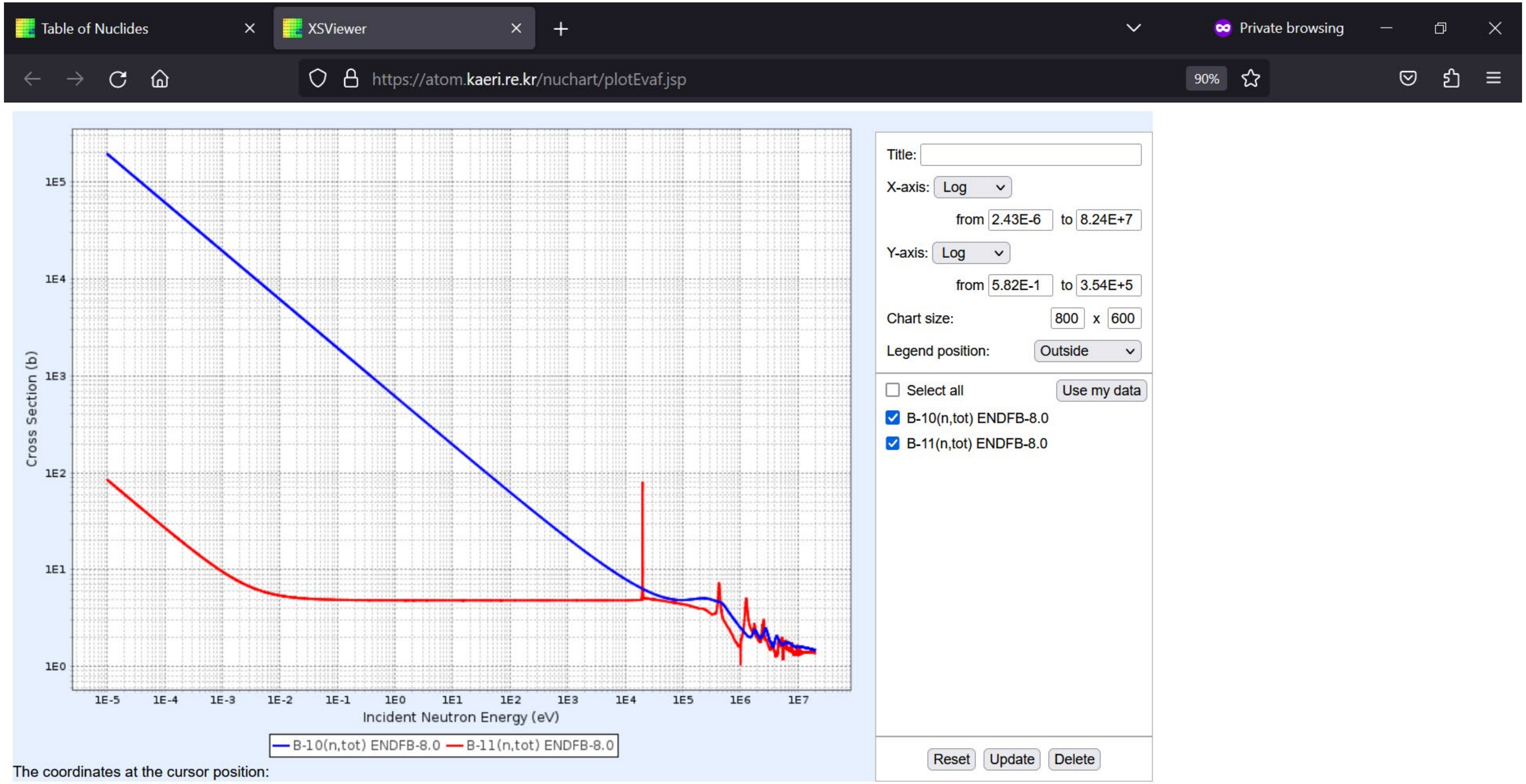

Cross-sections

- Neutron cross-sections are energy-dependent
  ⇒ Choice of detector material depends on the energy range of interest!
- Neutron cross-sections are isotope-dependent
  ⇒ must be a stable isotope
  ⇒ Choice of detector material depends on how abundant that isotope is, how cheap, how harmful etc. (life is full of compromises)
- Cross-sections >1000 barns tend to be useful

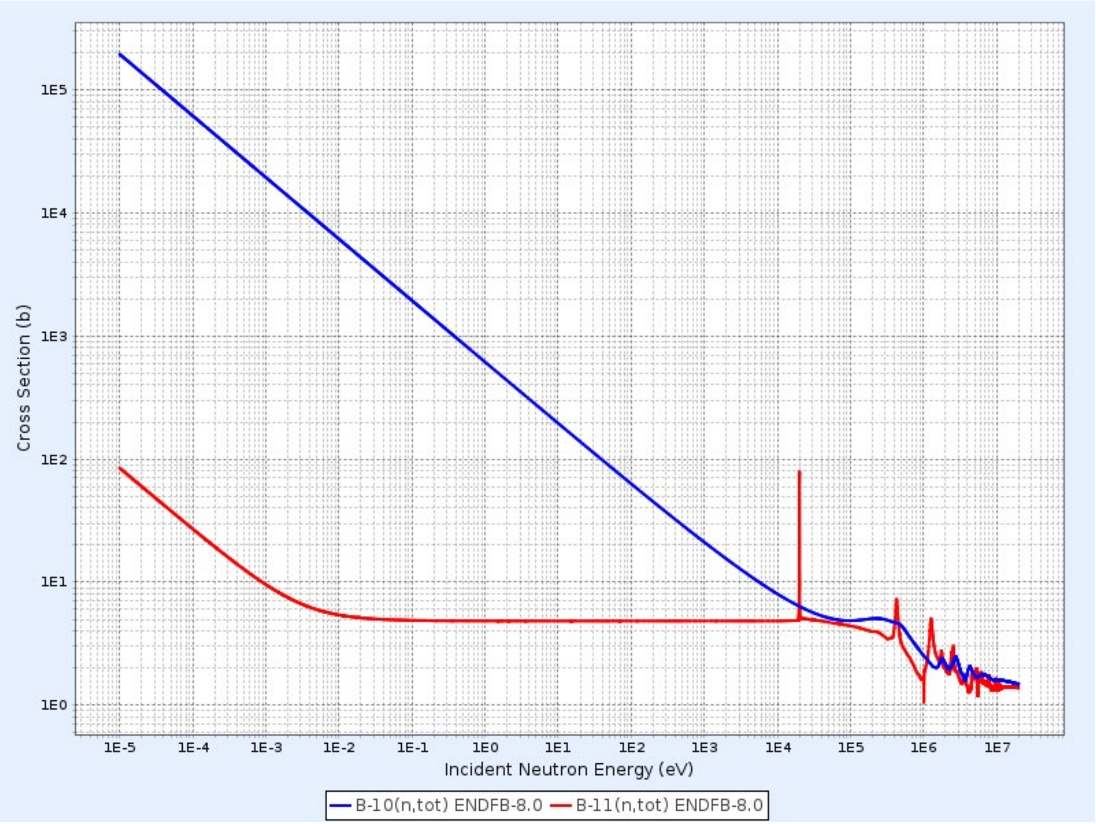

Home

B Find

5-B

Available Isotopes

B-6 (p-unstable)	B-7 (570ys)	B-8 (771.9ms)
B-9 (800zs)	B-10 (19.9%)	B-11 (80.1%)
B-12 (20.20ms)	B-13 (17.16ms)	B-14 (12.36ms)
B-15 (10.18ms)	B-16 (>4.6zs)	B-17 (5.08ms)
B-18	B-19 (2.92ms)	B-20 (>912.4ys)
B-21 (>760ys)		

Cross-sections

- Neutron cross-sections can be measured for different types of interactions
- For detection we typically care about capture reactions
- Total cross-section is a good start
- (n,α) tend to be good reactions for detectors
- For B-10, total cross-section up to ~100 keV is dominated by (n,α) $\Rightarrow$ therefore…

Neutron-induced Cross Sections

List of Evaluated Nuclear Data Libraries

ENDF/B-VIII.0	Full text
- Cross sections	
Total cross sections	Plot
Elastic cross sections	Plot
Nonelastic cross sections	Plot
Inelastic cross sections	Plot
(n,n_k) cross sections (click to expand)	
Capture cross sections	Plot
(n,p) cross sections	Plot
(n,d) cross sections	Plot
(n,α) cross sections	Plot
(n,t2α) cross sections	Plot
(n,p_k) cross sections (click to expand)	
(n,t_k) cross sections (click to expand)	
(n,α_k) cross sections (click to expand)	

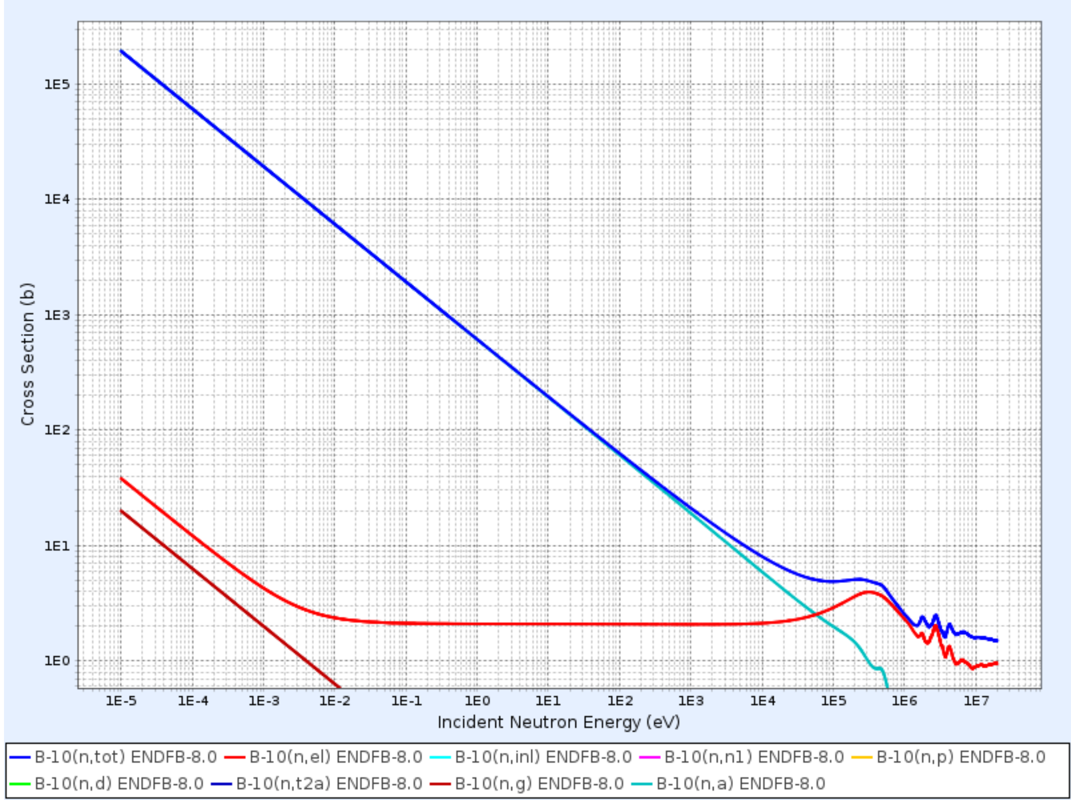

Boron-based detectors

$$
\begin{aligned}
{}^{10}\mathrm{B} + \mathrm{n} &\rightarrow {}^{7}\mathrm{Li} + {}^{4}\mathrm{He} + 2.79\ \mathrm{MeV} \quad (6\%) \\
{}^{10}\mathrm{B} + \mathrm{n} &\rightarrow {}^{7}\mathrm{Li}^{*} + {}^{4}\mathrm{He} + 2.31\ \mathrm{MeV} \quad (94\%) \\
&\qquad \downarrow \\
&\quad {}^{7}\mathrm{Li} + 480\ \mathrm{keV}
\end{aligned}
$$

- Energy release is kinetic energy of particles or γ
- Kinetic energy can ionize more particles
- In an electric field that can ionize more particles $\Rightarrow$ avalanche
- Avalanche of charged particles ultimately becomes measureable electric signal
  $\Rightarrow$ A neutron was detected! (or a γ, don’t be fooled)

Boron-based detector: “Tremsin detector” Multi-channel Plate TimePix Radiography Detector

- If a neutron hits a boron-doped glass plate with pores (“channels”), the energetic particles from the absorption reaction create free electrons
- With a vacuum around the plate and ~2keV electric field (under a few degrees angle to the pores), more electrons are ionized (think: photo-multiplier)
- Install multi-channel plate with vacuum and electric field in front of a TimePix chip $\Rightarrow$ ~10^6 electrons provide enough charge to be detected by a TimePix chip
- Detector provides x,y,t $\Rightarrow$ TOF radiography detector, 55 μm pixel size
- Pore size ~8 μm, angle 3°, diameter 33 mm
  $\Rightarrow$ No spread of signal by much more than pore size
  $\Rightarrow$ Good resolution
  $\Rightarrow$ Four TimePix chips cover 28x28mm^2
- This detector pioneered the field of energy-resolved neutron imaging (ERNI) and Bragg-edge radiography & tomography (BERT)
- Each pulsed neutron user facility has at least one!
- Significant γ sensitivity
- Technology originally developed for Hubble telescope (Space Science Laboratory at UC Berkeley)

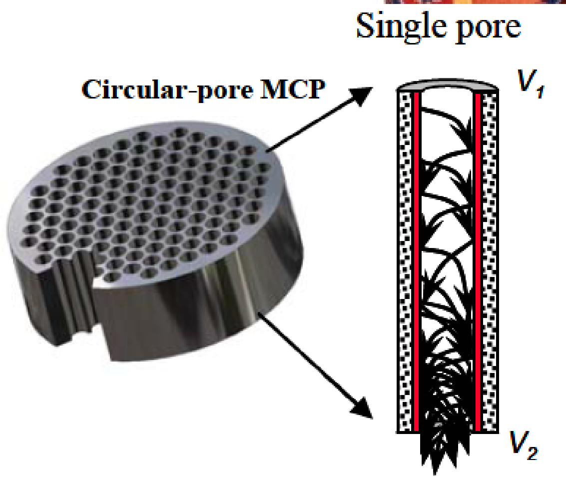

Figure 1. The principle of event amplification in a sensor with microchannel paltes. A single electron (created by photon,ion,neutron) at the pore is accelerated and creates an electron avalanche resulting in event gain up to 10^6.

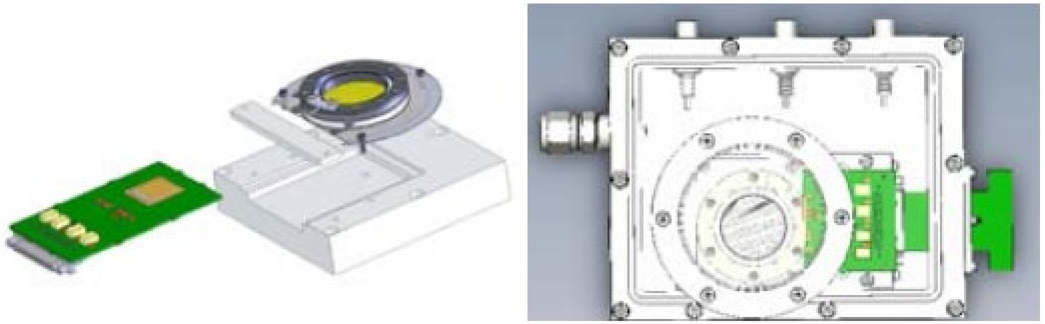

Figure 2. Schematic diagram of neutron the counting detector with MCPs and a Medipix/Timepix readout. Single chip active area 14x14 mm^2.

Tremsin, A.S., McPhate, J.B., Vallerga, J.V., Siegmund, O.H.W., Kockelmann, W., Steuwer, A. and Feller, W.B., 2011. High-resolution neutron counting sensor in strain mapping through transmission bragg edge diffraction. *IEEE Sensors Journal*, *11*(12), pp.3433-3436.

Boron-based detector: ERNI with Tremsin detector

- Some isotopes have so-called neutron absorption resonances
  $\Rightarrow$ cross-section changes from ~10 barns to >1000 barns for energy range of ~0.1 eV
- Allows to identify isotopes in a neutron beam but also to quantify the density from the known cross-section
- With 2D mapping, 3D tomography can be produced
- Energy-resolved neutron imaging requires transmission signal for each pixel
  $\Rightarrow$ requires efficient radiography detector

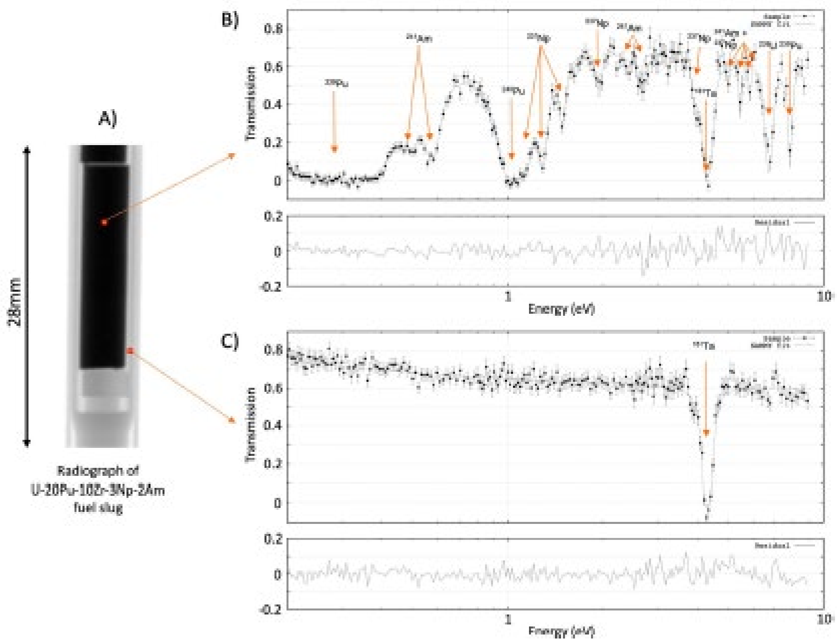

Figure 1. Thermal neutron radiograph (A) with single pixel data for isotope concentration measurement with a fit of the transmission data inside (B) and outside (C) the sample. Arrows mark the resonances of several isotopes and the difference curves between experimental data and fit are shown below.

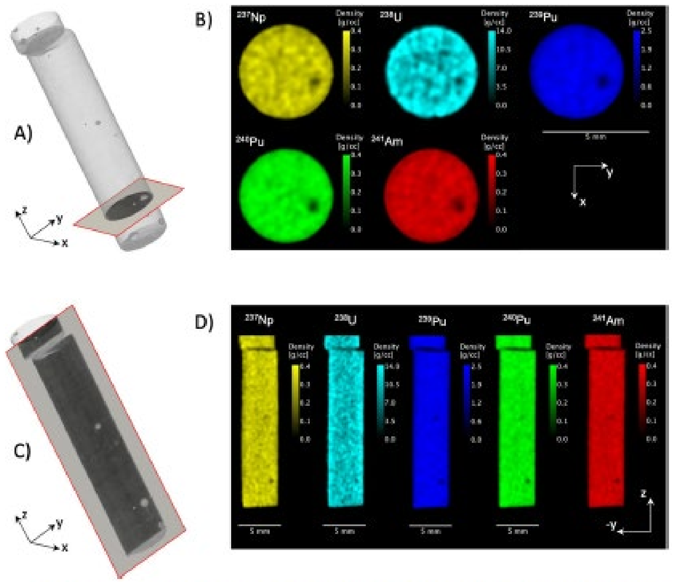

Figure 2. Volumetric reconstruction using epithermal neutrons of the U-20Pu-10Zr-3Np-2Am sample with indicated region in red for CT slices of the volumetric densities of individual isotopes. Slices normal to the cylinder axis in (A) with corresponding isotope densities shown in (B) and slices parallel to the cylinder axis in (C) with corresponding isotope densities shown in (D), respectively.

Losko, Adrian Simon, and S. C. Vogel. "3D isotope density measurements by energy-resolved neutron imaging." Scientific Reports 12.1 (2022): 6648.

Boron-based detector: BERT with Tremsin detector

- Bragg's Law: Diffraction happens if and only if
  $$\lambda=2d\sin\vartheta$$
- Bragg-edges are formed in the transmitted signal when a set of lattice planes is excluded from Bragg-scattering because $\lambda>2d$
  (λ grows with time-of-flight at a pulsed source, $\sin\vartheta$ cannot be greater than 1)
- Can be used to discriminate e.g. bcc α-Fe from fcc γ-Fe (ferrite/austenite in steel)
  $\Rightarrow$ density difference is ~2%, difficult to resove with e.g. X-ray CT
- Bragg-edge radiography and tomography

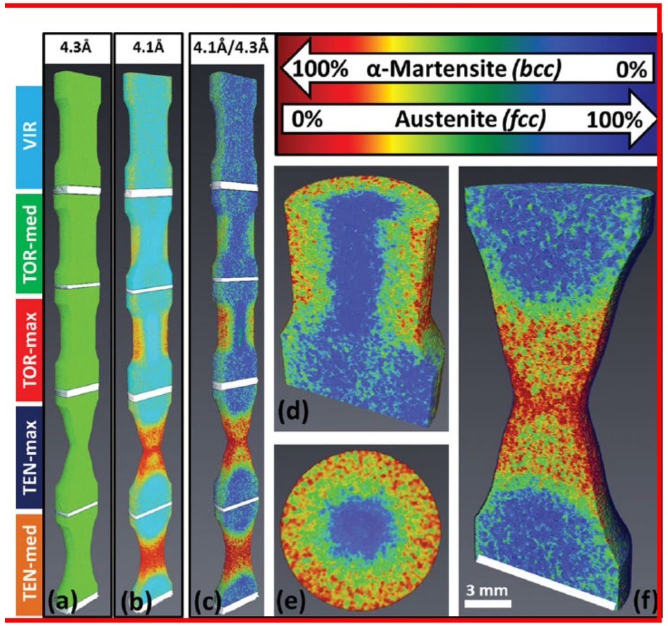

Figure 2. Phase Reconstruction in 3D. a,b) Center slice of the tomographic reconstruction of the five samples. Samples were cut to a region around the gauge area of virgin and deformed specimens and assembled together for simultaneous neutron tomography at wavelengths before (4.1 Å) and after (4.3 Å) the 'Bragg cut-off' corresponding to the austenitic phase. c–f) The reconstructed data sets were divided (4.1 Å/4.3 Å), to accentuate the transmission intensities due to Bragg diffraction and phase fractions were quantified. d,e) The radial dependence of the phase transformation in the torsion sample (TOR-max) is clearly visible in the tomographic reconstruction when viewing the cross section. f) Close-up of the tensile sample (TEN-max) showing that the necking region and regions close to the gauge area surface have the highest martensitic phase contents.

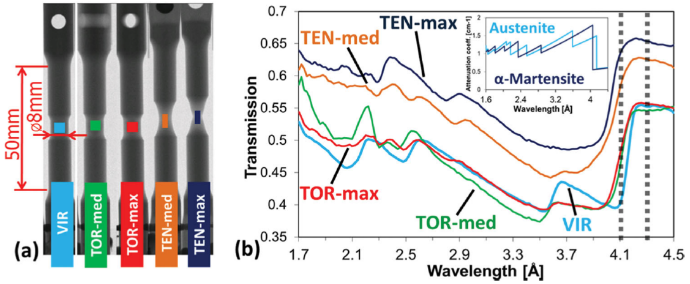

Figure 1. Transmission image and transmission spectra: a) Radiograph of samples with region of interest (ROI) depicted, which was used for the plot in Figure 1b. b) Bragg edge transmission spectra (131 mono-energetic radiographic projections between 1.7 Å and 4.5 Å with an exposure time of 240 seconds/projection) for the center gauge area of the five samples. The non-deformed sample "VIR" is purely austenitic, and only Bragg edges corresponding to austenite are visible. The center of tensile sample "TEN-max" is fully transformed to martensite (compare to theoretical attenuation coefficients depicted in inset and Figure S1) while "TEN-med" is only partially transformed over the selected ROI. The two torsion samples show Bragg edges of both crystallographic phases in the gauge area, which is anticipated, as the center of the sample is not expected to transform to martensite since the applied shear stress there is zero; hence tomographic reconstruction is needed for further quantification. Investigating regions outside the gauge area, the Bragg edge spectra are identical to those of the virgin sample, proving that no (significant) deformation occurred. The dotted vertical lines indicate the wavelengths where tomographic scans were performed.

Woracek, Robin, et al. "3D mapping of crystallographic phase distribution using energy-selective neutron tomography." Adv. Mater 26.24 (2014): 4069-4073.

Boron-based detector:
High count rate liquid scintillator detector

- Absorption cross-section of B-10 at 10 keV neutron energy has dropped to <10 barns
- Trick: Slow down a 10 keV neutron to 10 eV
  $\Rightarrow$ cross-section back to >200 barns
- Slow down = moderation $\Rightarrow$ add H to the scintillator
  $\Rightarrow$ trimethyl benzene solvent loaded with B-10-enriched trimethyl borate $C_3H_9BO_3$
- Fill a 43 cm diameter, 4 cm thick tank with that, view the downstream side with 55 photo-multiplier tubes
  $\Rightarrow$ 500 MHz counting event rate
  $\Rightarrow$ efficiency of 95%, 85%, and 71% at neutron energies of 10, 100 and 1000 eV, respectively
  (Tremsin detector: ~70% and 50% at 0.005eV and 0.025 eV, respectively)

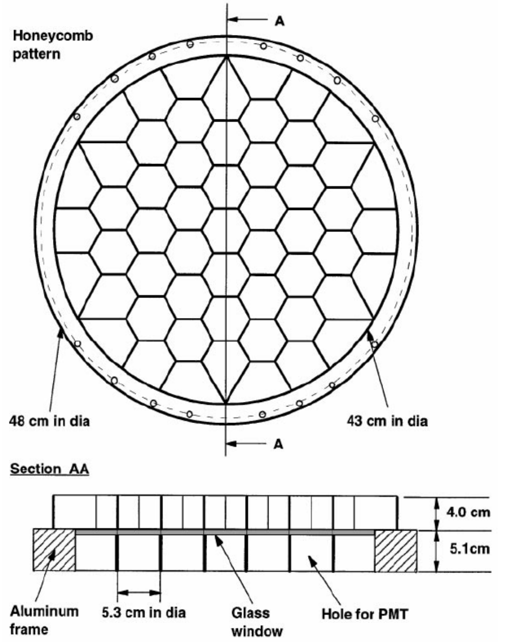

Fig. 2. The 55-module ^{10}B-loaded liquid scintillation detector. The upper part of the figure shows the honeycomb pattern of the cell arrangement. Each cell is viewed by a 5-cm diameter PMP. The lower part of the figure shows the cross sectional view of the scintillation container without the aluminium entry window flange.

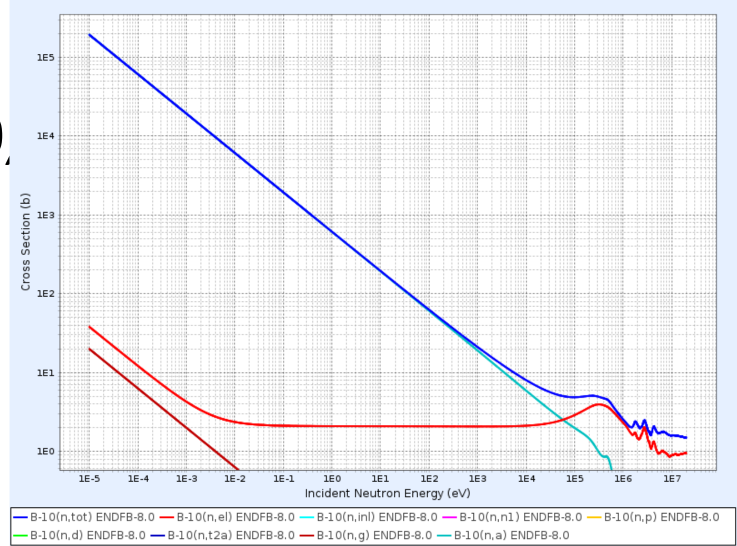

Yen, Yi-Fen, et al. "A high-rate 10B-loaded liquid scintillation detector for parity-violation studies in neutron resonances." *Nuclear Instruments and Methods in Physics Research Section A: Accelerators, Spectrometers, Detectors and Associated Equipment* 447.3 (2000): 476-489.

Boron-based detector:
Nuclear physics with liquid scintillator detector

- Parity violation can be observed by detailed neutron absorption resonance line profile analysis
- For some isotopes, the relevant resonances are >100 eV, e.g. Sb-121, Sb-123
  ⇒ Neutron flux provided by water moderator is low at those energies
  ⇒ Cannot afford to miss neutrons
  ⇒ Need efficient detectors where B-10 has dropped to <50 barns
  ⇒ Used 500 MHz liquid scintillator detector
- Also could use the <1ns pulses of a LDNS!

Matsuda, Y., et al. "Parity violation in neutron resonances of antimony and iodine." *Physical Review C* 64.1 (2001): 015501.

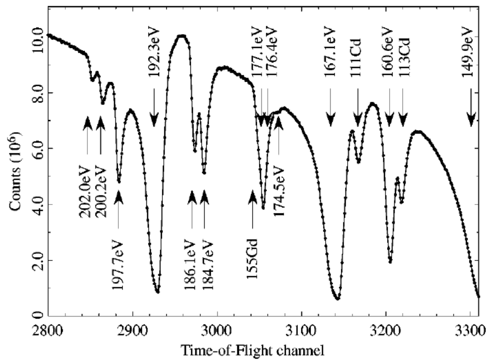

FIG. 1. Neutron time-of-flight spectrum for transmission in natural antimony in the energy range 150–210 eV. The resonances indicated are all *s*-wave resonances.

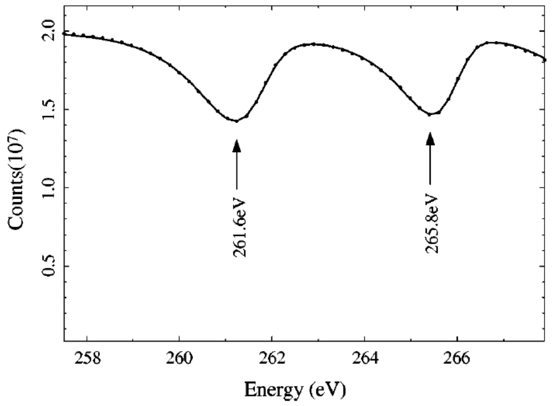

FIG. 2. Neutron time-of-flight spectrum for transmission in natural antimony shown on an expanded energy scale near 260 eV. The solid line represents the fit obtained with the analysis code FITXS. Note that the asymmetric line shapes of the two *p*-wave resonances are well reproduced.

Boron-based detector: Materials science with liquid scintillator detector

- Bragg-edges can be detected quicker than diffraction peaks (at the cost of having to watch a small change in a large signal)
- Time-sensitive phenomena such as phase transformations or chemical reactions can be probed with Bragg-edges
- Reduction of nickel-oxide to nickel is an example
  - Data was collected with 30 seconds count time using the liquid scintillator detector
  - Weight fractions and lattice parameters can be derived from Bragg-edges
  - Could be done much nicer today with imaging detector

Vogel, S., et al. "In-situ investigation of the reduction of NiO by a neutron transmission method." Materials Science and Engineering: A 333.1-2 (2002): 1-9.

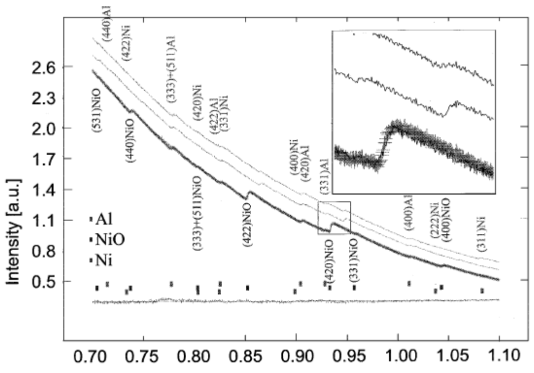

Fig. 1. Bragg-edge transmission patterns at 1100 °C after 10.75 h in the reducing atmosphere (top), at 1100 °C before reduction (middle curve) and at room temperature (bottom curve). Tick marks indicate (from top to bottom) edge positions of Al (from furnace end-caps), NiO and Ni, respectively. The positions of Al and NiO reflections are calculated for room temperature while those of the Ni are for 1100 °C. The difference curve for the fit of the room-temperature pattern is shown in the same scale at the bottom of the figure.

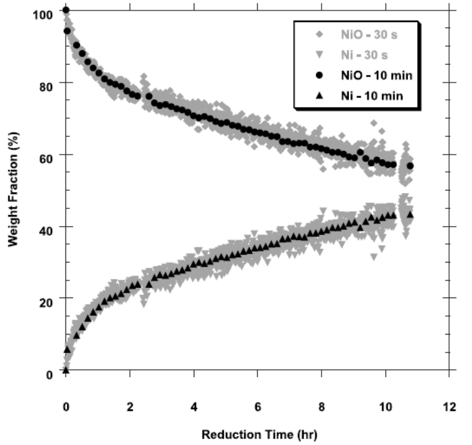

Fig. 3. Weight fraction evolution of NiO and Ni during reduction at 1100 °C. For clarity, only the 30 s and 10 min time integration data are shown. An increase in scatter as the time resolution increases is apparent. The interruptions in data (e.g. around 10 h) are due to poor neutron beam quality, which leads to poor counting statistics at the detector.

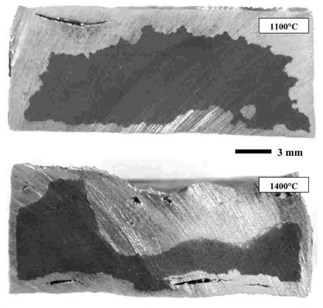

Fig. 8. Optical micrographs of the specimen cross-sections. The light gray regions are Ni and dark gray areas are NiO. Some internal cracks and voids are seen in black.

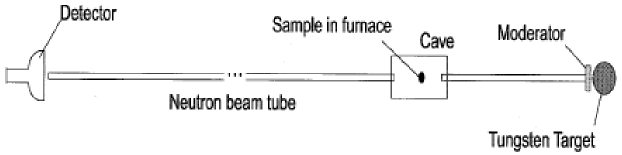

Fig. 2. Schematic of the experimental setup used at Flight Path 5 of LANSCE.

Integrated Circuits contain B-10

- Neutron absorption reactions can happen in integrated circuits containing B-10
- If spatial location of a bit in e.g. RAM module is known, a neutron detector can be built from RAM modules (has been demonstrated, but not overly useful…)

IEEE TRANSACTIONS ON NUCLEAR SCIENCE, VOL. 67, NO. 1, JANUARY 2020 29

Thermal Neutron-Induced Single-Event Upsets in Microcontrollers Containing Boron-10

Elizabeth C. Auden, *Member, IEEE*, Heather M. Quinn, *Senior Member, IEEE*, Stephen A. Wender, John M. O'Donnell, Paul W. Lisowski, Jeffrey S. George, *Senior Member, IEEE*, Ning Xu, Dolores A. Black, *Senior Member, IEEE*, and Jeffrey D. Black, *Senior Member, IEEE*

***Abstract*—Single-event upsets (SEUs) were measured in thermal neutron-irradiated microcontrollers with 65- and 130-nm-node static random-access memories (SRAMs). The suspected upset mechanism is charge deposition from the energetic byproducts of ^{10}B thermal neutron capture. Although elemental analysis confirmed that both microcontrollers contain ^{10}B, only the 65-nm node microcontroller exhibited a strong response to thermal neutrons. Monte Carlo simulations were performed to investigate the effects of ^{11}B enrichment on thermal neutron-induced SEUs in a 65-nm SRAM node when boron is present in the *p*-type well, *p*-type source and drain, or tungsten plug. Simulations indicate that the byproducts of ^{10}B(n, α) ^{7}Li reactions are capable of generating sufficient charge to upset a 65-nm SRAM. The highest amount of charge deposition from ^{10}B(n, α) ^{7}Li reaction byproducts occurs when natural boron is used to dope the *p*-type source and drain regions. Simulations also show that the SEU cross section is nonnegligible when ^{11}B-enriched boron is used for doping.**

***Index Terms*—Microcontrollers, neutrons, radiation effects, semiconductor device doping, semiconductor device modeling, single-event effects (SEEs), static random access memory (SRAM) cells.**

The literature contains many reports of thermal neutron-induced SEEs for components containing ^{10}B, such as static random access memories (SRAMs), dynamic random access memories (DRAMs), and power metal–oxide–semiconductor field effect transistors (MOSFETs), but there is little information about thermal neutron-induced SEEs in microcontrollers. BPSG was the first source of ^{10}B to be associated with thermal neutron-induced SEEs in semiconductor components. BPSG can be inserted as an insulating layer between metallization layers during fabrication. BPSG is attractive to the manufacturing process because it has a lower melting point than silicon dioxide. Thermal neutron-induced SEEs were reported for DRAMs and SRAMs containing BPSG in [1]–[3], and the 20% abundance of ^{10}B in the natural boron used in BPSG layers was identified as the culprit. Semiconductor foundries started to leave BPSG out of the manufacturing process at the 180-nm node and below, yet thermal neutron-induced SEEs have continued to be reported for modern components suspected to

Helium-3

2-He

Available Isotopes

He-3 (0.000134%)	He-4 (99.999866%)	He-5 (602ys)
He-6 (806.92ms)	He-7 (2.51zs)	He-8 (119.5ms)
He-9 (2.5zs)	He-10 (260ys)	

- Low concentration in natural abundance
  - Needs to be enriched
  - Makes it more expensive than a material that can be used in natural composition
- He-3 is only stable isotope of any element with more protons than neutrons

$$^{3}\mathrm{He} + \mathrm{n} \quad \rightarrow \quad \mathrm{T} + \mathrm{p} + 0.765\ \mathrm{MeV}$$

- Tritium decays back into He-3 $\Rightarrow$ Life-time is not limited by "detecting"
- Slightly higher cross-section than B-10 – but B-10 can be a solid, helium gas at room temperature $\Rightarrow$ ~1,000 less dense

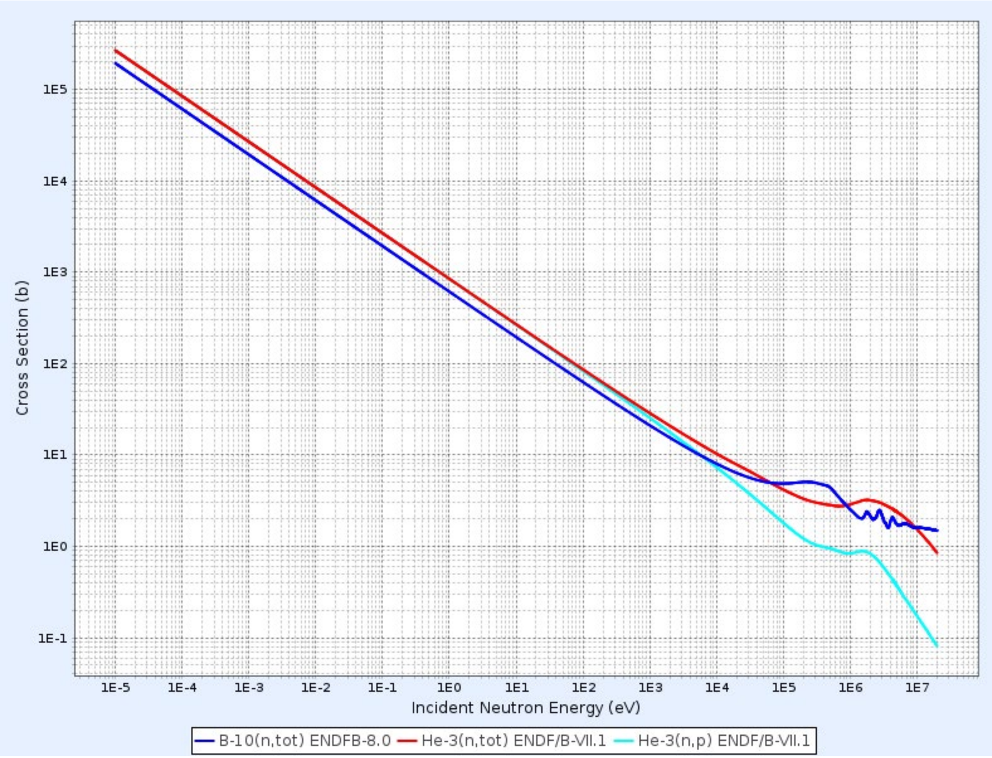

He-3 neutron detector tubes

- He-3 enriched to ~20 at%. In the gas
- Principle of a Geiger-Müller counter:
  - Capture happens
  - Energetic particles ionize gas atoms
  - Ions and electrons are accelerated in 1-2 kV electric field and ionize more
  - Avalanche generates enough charge to provide measurable electrical signal
- Geiger-Müller counters also work with BF_3 gas detectors but He-3 is much less hazardous
- Neutron by itself does not ionize, needs to be captured
- Same for gammas $\Rightarrow$ low gamma sensitivity
- Container material typically aluminum or steel, gas pressure several atmospheres
- Diameters typically 10-50.8 mm (½ to 2` inch), lengths from 60 to 2000 mm
- Spatially resolved only along tube with run-time of electrical system
  $\Rightarrow$ often one tube is a large pixel
- Typically used for thermal neutron scattering/neutron diffraction
- Dead time

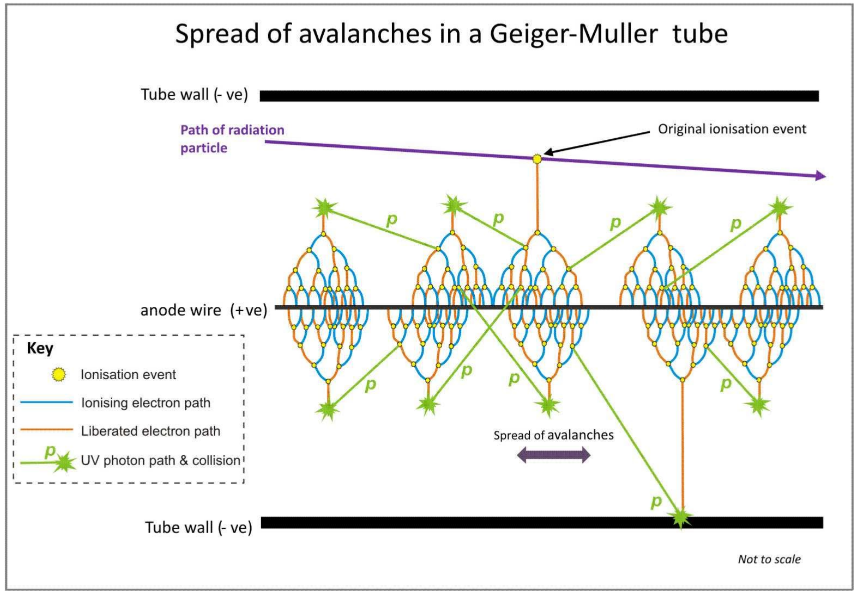

Figure 2.2 Tubes used in a proportional detector for large-area detectors. Source: Oak Ridge National Laboratory.

He-3 neutron detector tubes
Example: Diffractometer at LANSCE

- HIPPO: HIgh Pressure – Preferred Orientation
- Detector coverage: 4.9 m^2, 22.3% of 4π
  (1200 ^{3}He tubes on 53 panels)
- General purpose diffractometer
  - Crystal structure analysis
  - Texture measurements
  - Sample environments for temperature, stress, pressure, magnetic field etc.
- Measurement time for texture: 1-10 minutes
- Moderator-sample distance: 8.83 m
- Beam spot: 10 mm Ø
- Thermal flux: ~10^7 n/s/cm^2 Sample chamber: ~1m^3, 73.4cm ∅ opening
- How do you think the He-3 tubes are arranged for diffraction?

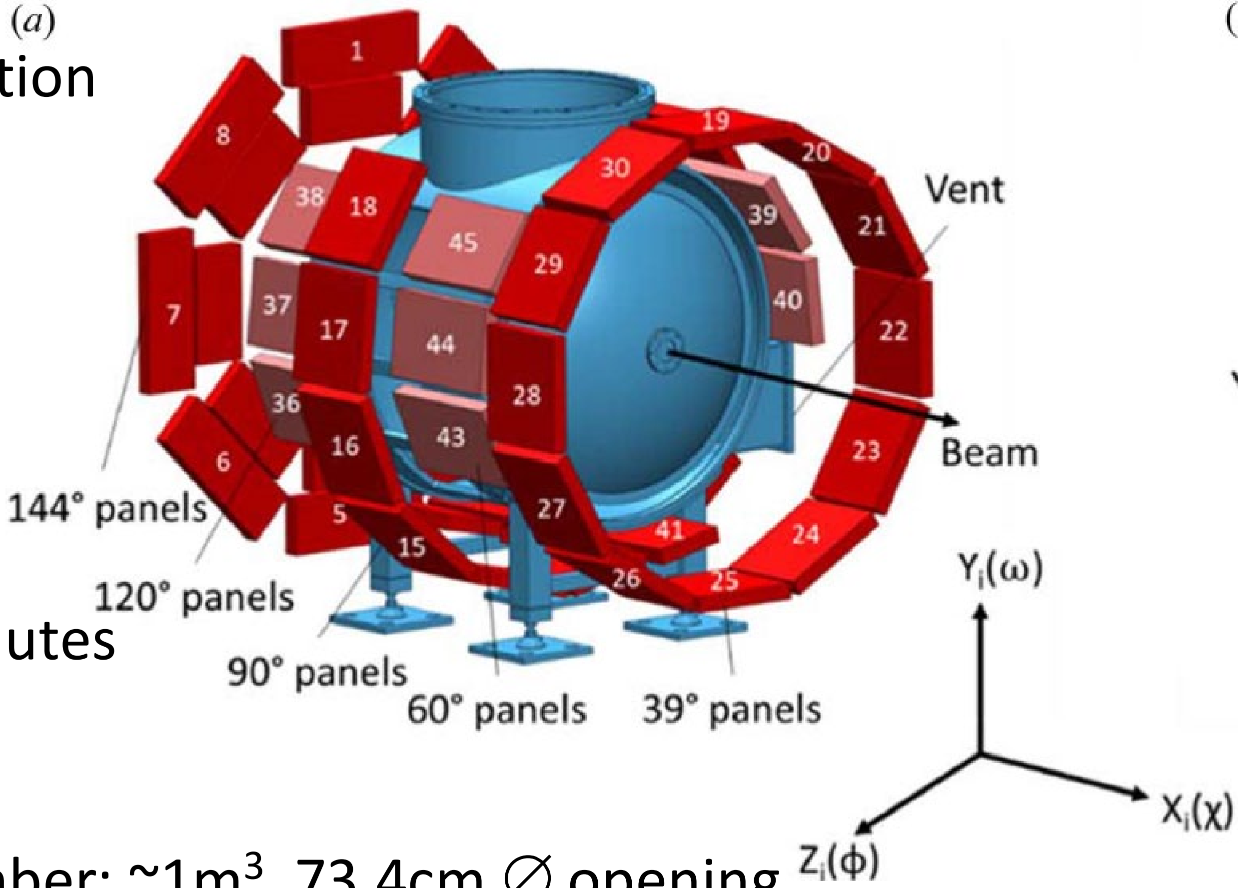

Wenk et al., NIM, ***515*** (2003) 575. Vogel et al., Powder Diffraction, **19** (2004) 65, Takajo & Vogel, J. Appl. Cryst. (2018). **51**, 895–900, Schmitt et al. J. Appl. Cryst. (2023). **56**, 1764–1775.

He-3 neutron detector tubes
Example: Diffractometer

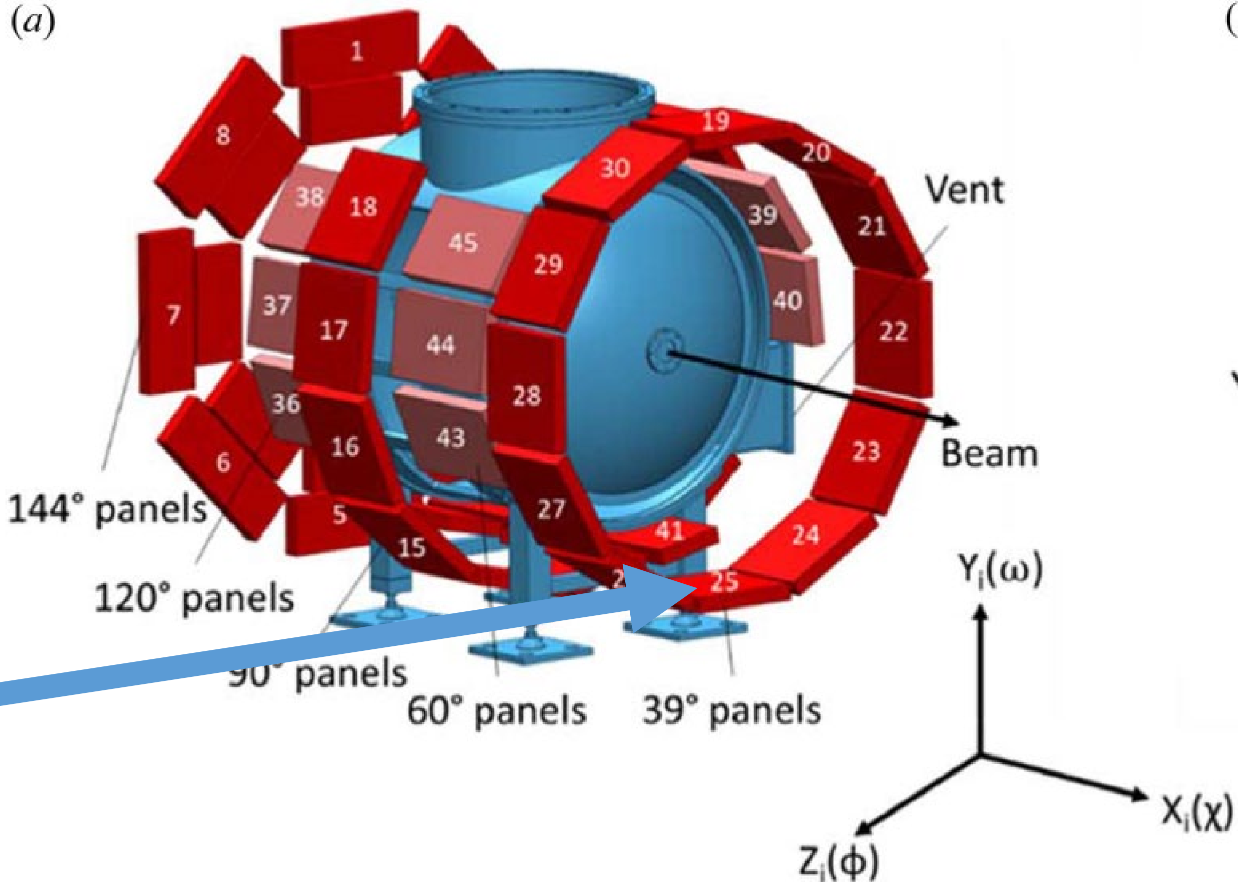

Wenk et al., NIM, ***515*** (2003) 575. Vogel et al., Powder Diffraction, **19** (2004) 65, Takajo & Vogel, J. Appl. Cryst. (2018). **51**, 895–900, Schmitt et al. J. Appl. Cryst. (2023). **56**, 1764–1775.

He-3 neutron detector tubes
Example: Diffractometer

- Material characterization using powder diffraction: phase fractions, lattice parameters, crystal structures etc.
- ~ 0.5cm^3 Quartz, **183 pulses@90μA (9 seconds…)**
- a=4.9160(2), c=5.4075(4)
- statistical uncertainty < 10^{-4}
  $\Rightarrow$ thermal expansion 10^{-5}/K
  $\Rightarrow$ useful experiments can be done

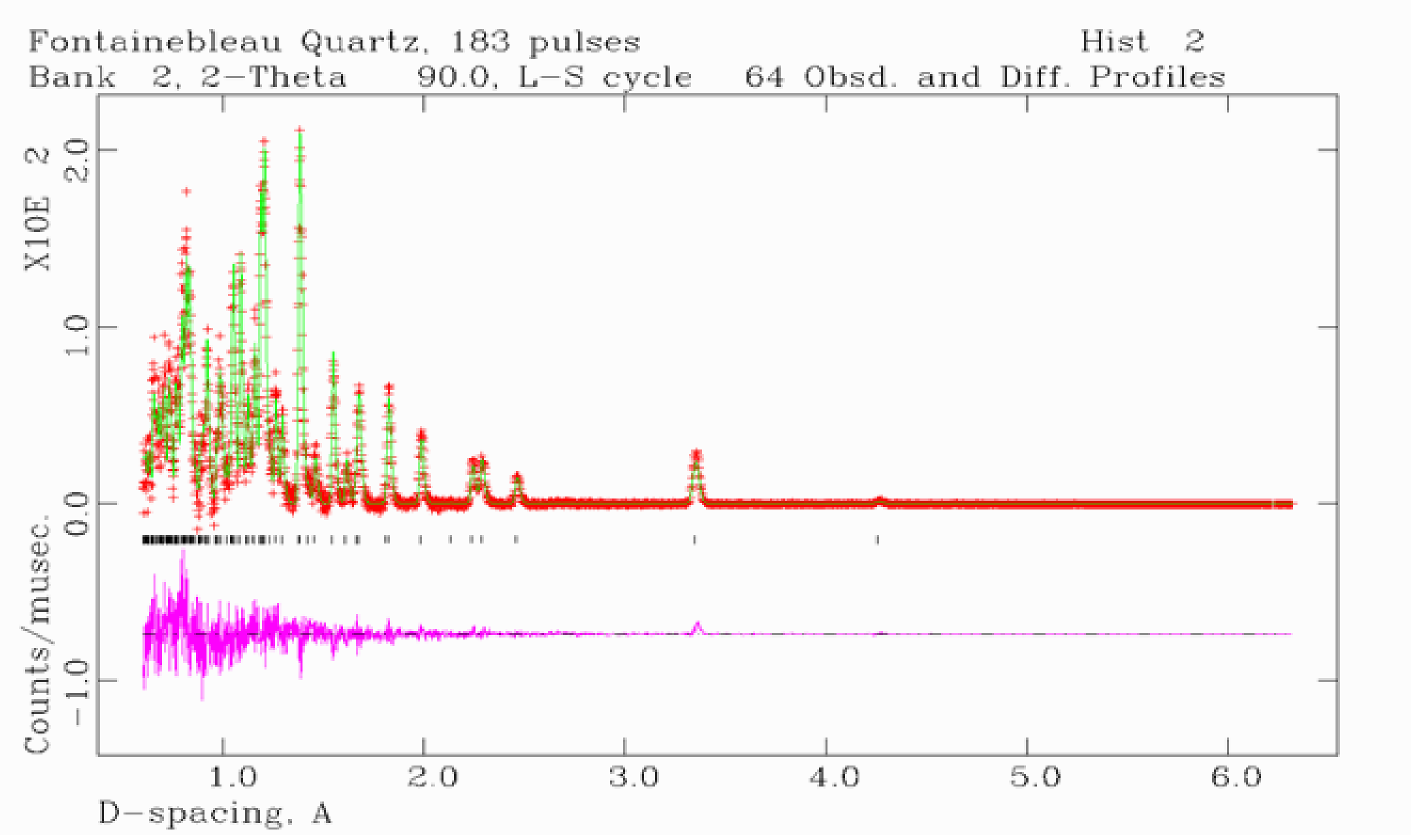

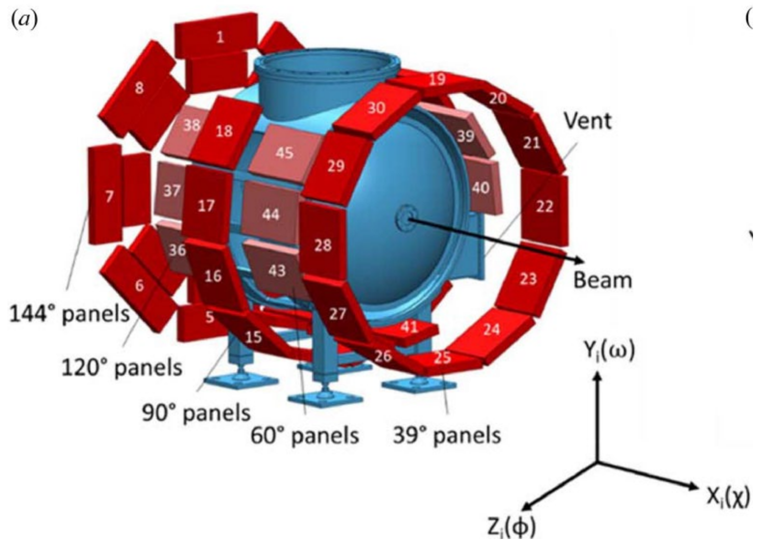

<1 minute count time useful $\Rightarrow$ HIPPO detector coverage at a source providing ~10^5 n/s/cm^2 would still allow "overnight measurements" like lab-XRD
$\Rightarrow$ large detector coverage can recover weaker source flux!

He-3 neutron detector tubes Example: Tinman

- Tinman:
  - Two He-3 detector tubes, one bare, one Cd shielded (thermal and epithermal neutrons)
  - High voltage supply, readout electronics including storage that can operate autonomously in aircraft

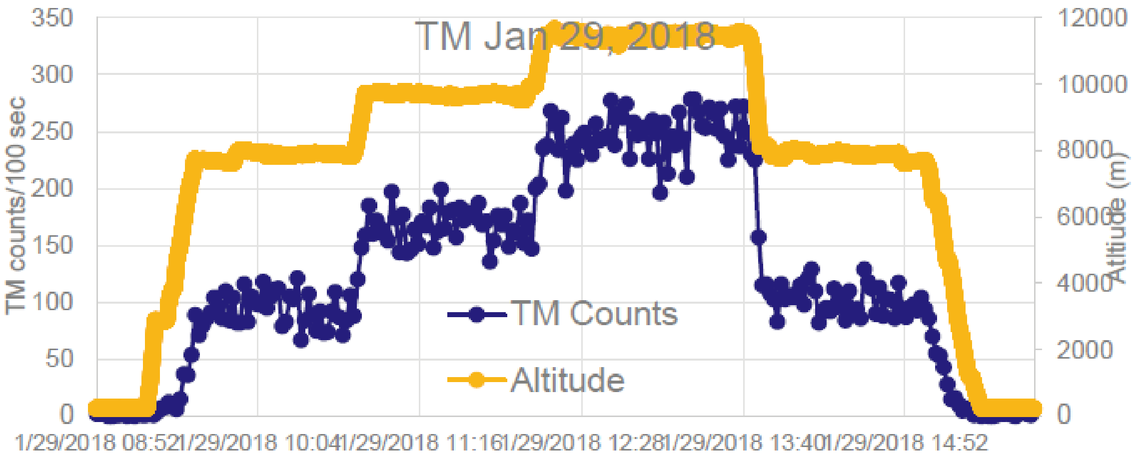

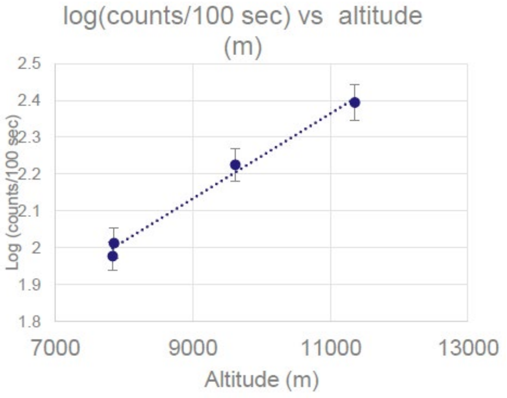

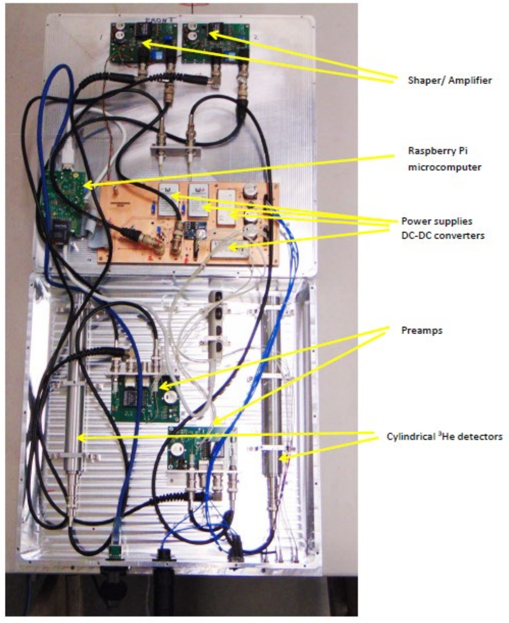

Figure 5. Inside of the Tin-II thermal-neutron detector. The Raspberry Pi microcomputer, the power supplies, the pre-amps and the discriminator circuits are attached to the lid of the box. The cylindrical ^{3}He detectors and the Shaper/Amplifiers are mounted to the bottom of the box. In this picture, the cadmium shield is not on the detector.

Wender et al., Report on the Tin-II Thermal Neutron Detector, LA-UR2019-10-24, Wender, TINMAN Thermal Neutron Detector for Aircraft, LA-UR 2021-05-14

He-3 neutron detector tubes Example: Tinman

- Tinman flew in ER-2 airplane
- ER-2 is civilian version of U-2 spy plane
- Maximum altitude is classified
- Flew on 4 flights from NASA Armstrong Flight Research Center in Palmdale, CA

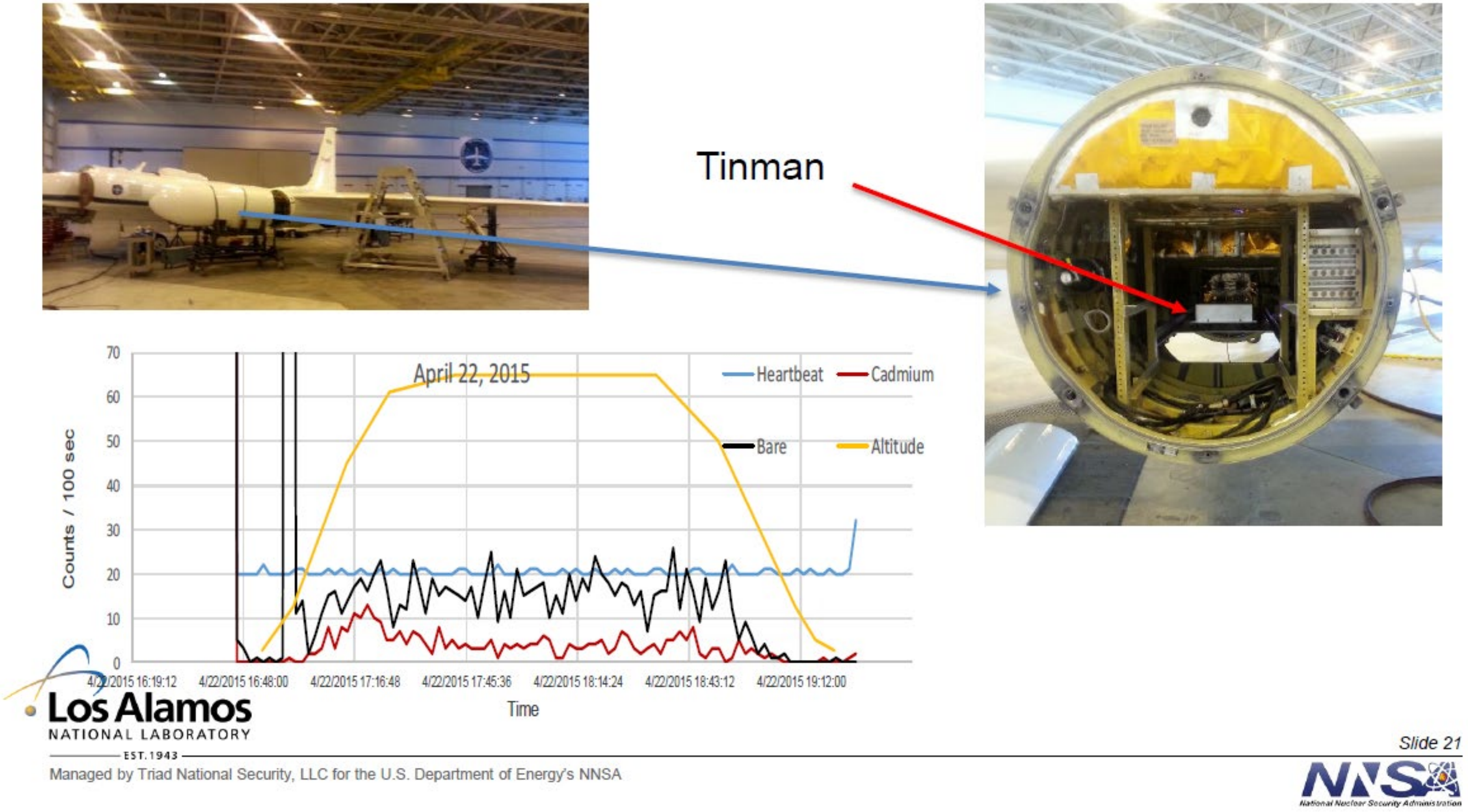

He-3 neutron detector tubes Example: Tinman

- Why care?

Figure 5. *This shows a large high-performance computer at Los Alamos National Laboratory. This is typical of large data centers, which can be vulnerable to thermal neutrons causing SEE.*

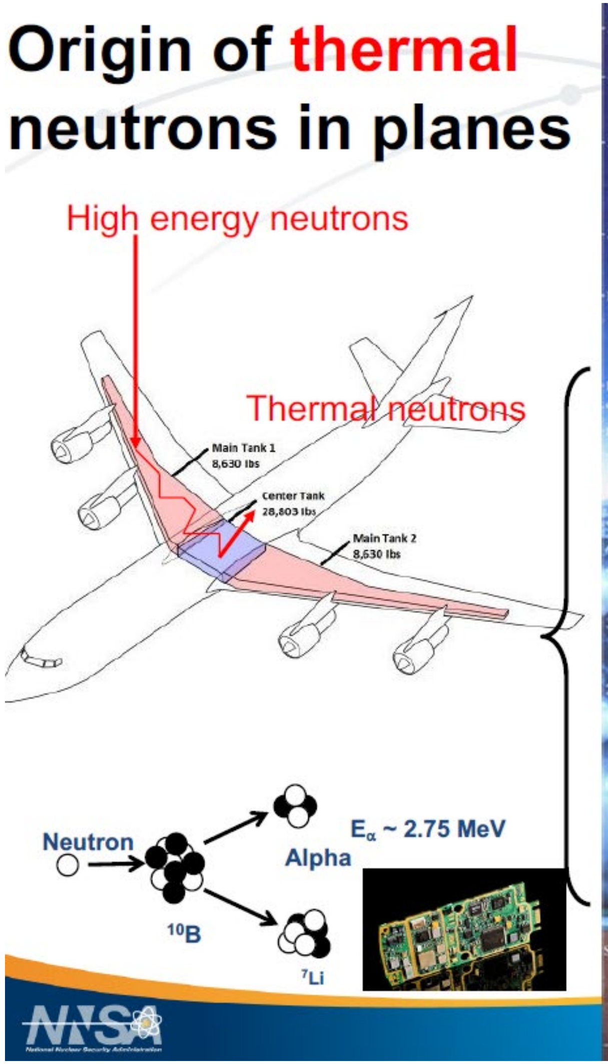

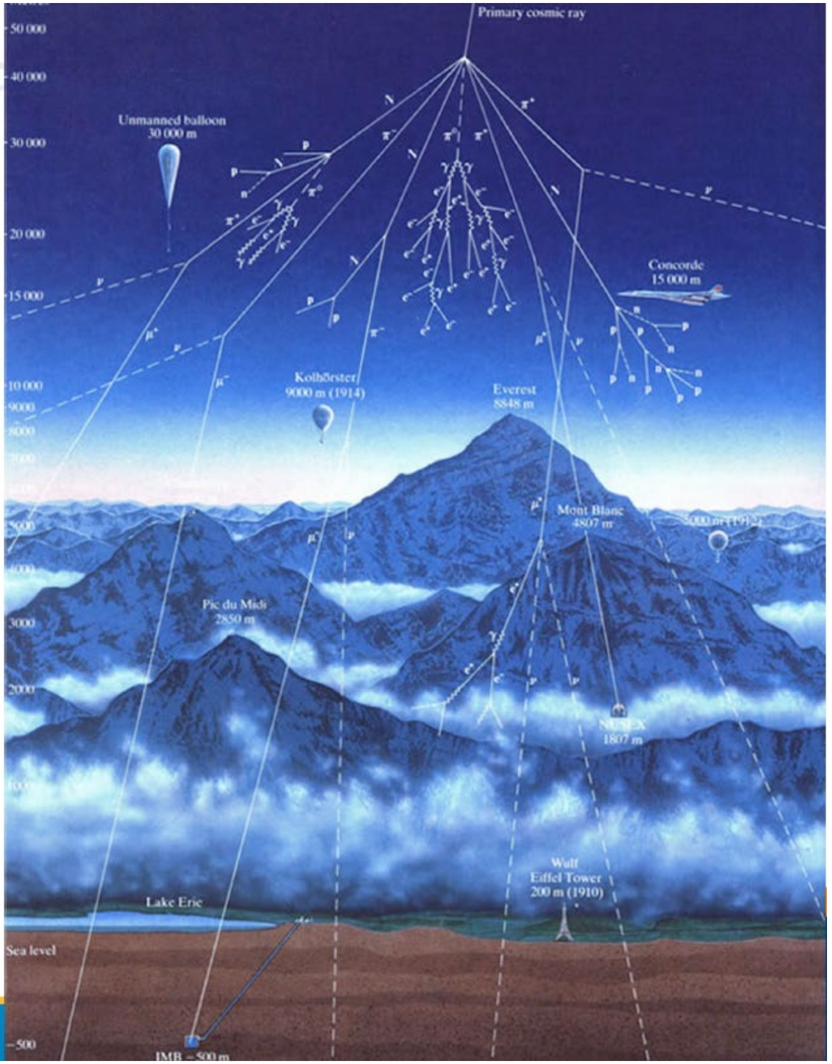

Novicki et al., Thermal neutron flux characterization at aircraft altitudes with the TinMan Detector in NASA aircraft, LA-UR2018-08-22,
Wender, TINMAN Thermal Neutron Detector for Aircraft, LA-UR 2021-05-14

He-3 neutron detector tubes
Example: Beam Monitors

- Measurement of source output needs calibrated, well understood beam monitors
- Neutron facilities utilize choppers to “chop” neutron beams for time-of-flight measurements
  $\Rightarrow$ Chopper performance needs to be monitored
- Determination of count time also requires beam monitors
- Beam monitors should…
  - …produce a sufficiently high count rate so good statistical accuracy may be obtained during the experiment
  - …produce a sufficiently low count rate that it will not contribute significantly to the dead time of the data acquisition system
  - …have good signal-to-noise characteristics
  - …not significantly perturb the incident beam or produce significant backgrounds for the primary experiment
  - …be relatively easy to set up and require a minimum of electronics to operate

Wender et al., Nucl. Instr. Meth. A (1993) **336** 226-231

He-3 neutron detector tubes
Example: Beam monitors

- Beam monitor: Vanadium foil in direct beam surrounded by He-3 detectors
- Vanadium scatters neutrons out of incident beam into He-3 detectors
- Number of counts provides measure for incident flux
- European Spallation Source is Lund has ~3ms long neutron pulses (LANSCE, ISIS, J-PARC: <1 μs)
  ⇒ need choppers for TOF
  ⇒ Each beamline has multiple choppers
  ⇒ Performance monitoring is an issue
  ⇒ Beam monitors are important

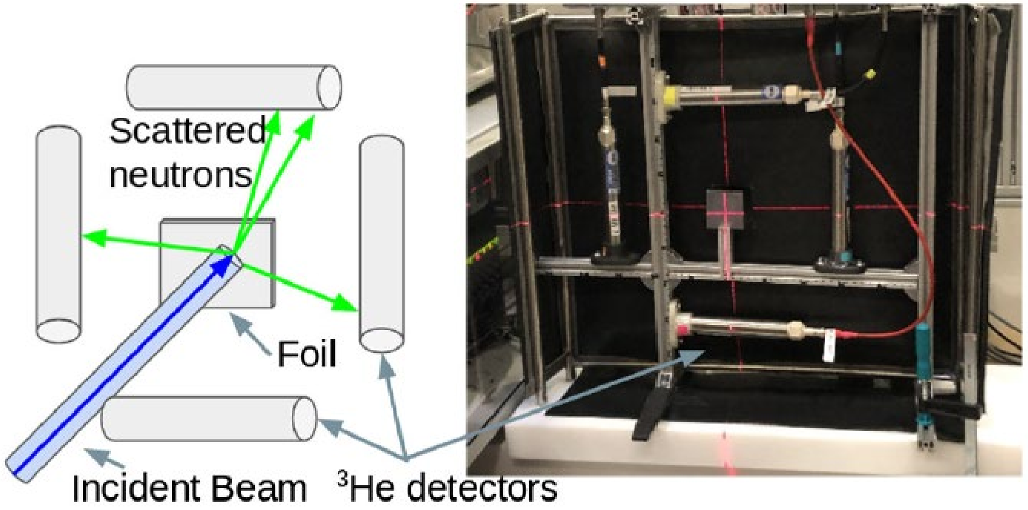

FIG. 3. Isotropic quasiparasitic beam monitor concept. The thin foil is placed in the beam of neutrons (denoted by the blue line). Small percentage of the neutrons are scattered from the foil (denoted by the green line). Left: Conceptual cartoon. Right: Photo of the experimental setup for the measurements. The laser cross shows the center of the neutron beam path.

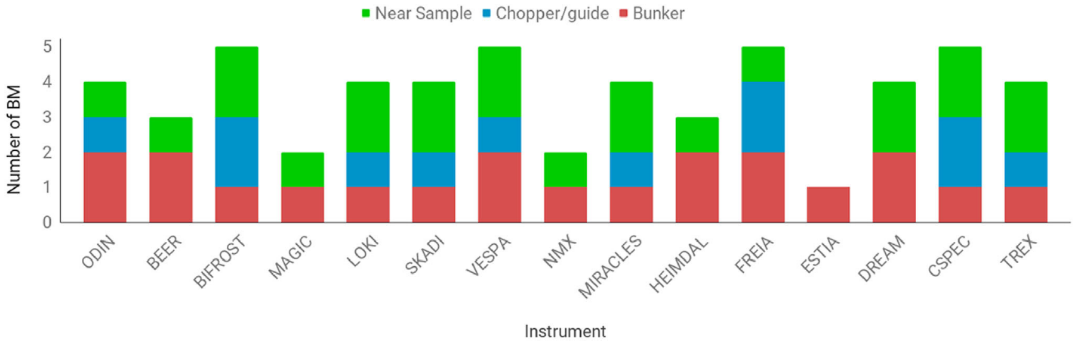

FIG. 1. The number of beam monitors anticipated to be required by the ESS instruments as of January 2020. The beam monitors are categorised into those near (before or after) the sample, along the neutron guides or next to choppers, or close to the beam extraction from the moderator in the "bunker" region.

Maulerova et al., Phys. Rev. Acc. & Beams (2020) **23** 072901

He-3 neutron detector tubes Example: Beam monitors

- Why vanadium?
  ⇒ Practically only incoherent scattering
  ⇒ ~constant from 1 meV to 100 eV
  ⇒ Low absorption
  ⇒ easy to handle
- Calibration with fission chamber

23-V

Available Isotopes

V-39	V-40	V-41
V-42	V-43 (79.3ms)	V-44 (111ms)
V-45 (547ms)	V-46 (422.62ms)	V-47 (32.6m)
V-48 (15.9735d)	V-49 (330d)	V-50 (0.250%)
V-51 (99.750%)	V-52 (3.743m)	V-53 (1.543m)
V-54 (49.8s)	V-55 (6.54s)	V-56 (216ms)
V-57 (350ms)	V-58 (191ms)	V-59 (95ms)
V-60 (122ms)	V-61 (48.2ms)	V-62 (33.6ms)
V-63 (19.6ms)	V-64 (15ms)	V-65 (14#ms)
V-66 (10#ms)	V-67 (8#ms)	

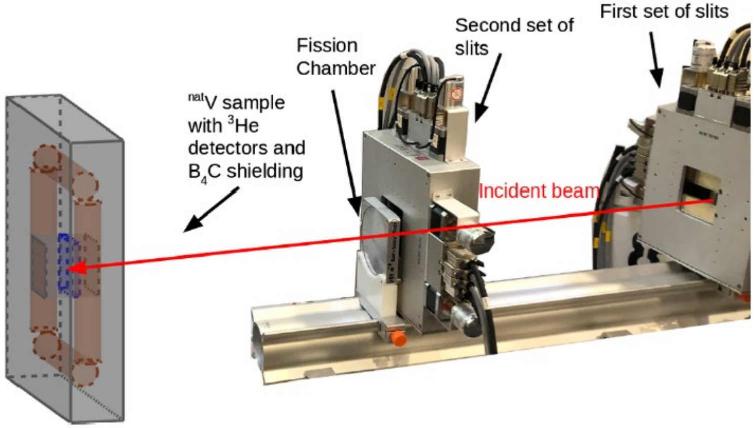

FIG. 4. Experimental setup on the beam line at V17. The incident beam (red) passes from the right to the left through two sets of (x,y) slits and a fission chamber before striking the ^{nat}V sample (blue).

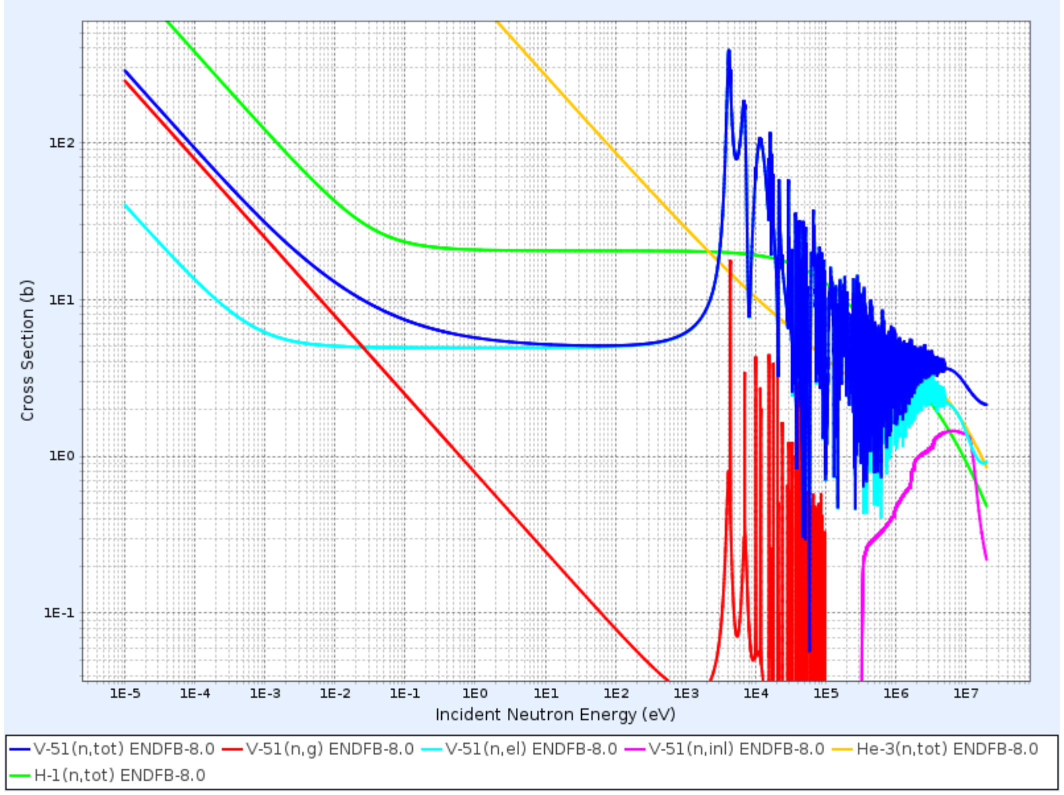

Maulerova et al., Phys. Rev. Acc. & Beams (2020) **23** 072901

U-238/235: Fission Chamber

- Fission chamber is a beam monitor that can provide absolute neutron flux while removing only negligible amount of neutrons
- Fission cross-sections are very well known
  $\Rightarrow$ with controlled thickness flux can be measured
  $\Rightarrow$ α particle spectroscopy can be used to measure areal density of uranium
- Absolute flux is needed e.g. for cross-section measurements
- Works for all neutron energies (with different coatings, e.g. more U-238 for MeV neutrons with fission threshold of ~1.5 MeV to avoid detection of previous pulse neutrons)

92-U

Available Isotopes

U-215 (1.4ms)	U-216 (6.9ms)	U-217 (850us)
U-218 (354us)	U-219 (60us)	U-220 (60#ns)
U-221 (660ns)	U-222 (4.7us)	U-223 (65us)
U-224 (396us)	U-225 (62ms)	U-226 (269ms)
U-227 (1.1m)	U-228 (9.1m)	U-229 (57.8m)
U-230 (20.23d)	U-231 (4.2d)	U-232 (68.9y)
U-233 (159.19ky)	U-234 (0.0054%)	U-235 (0.7204%)
U-236 (23.42My)	U-237 (6.752d)	U-238 (99.2742%)
U-239 (23.45m)	U-240 (14.1h)	U-241 (4#m)
U-242 (16.8m)	U-243 (16#m)	

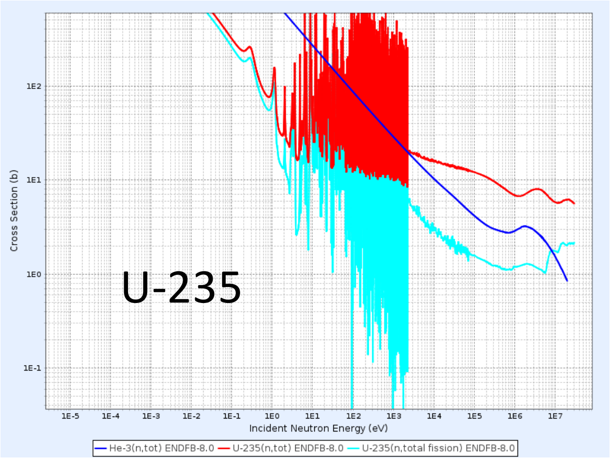

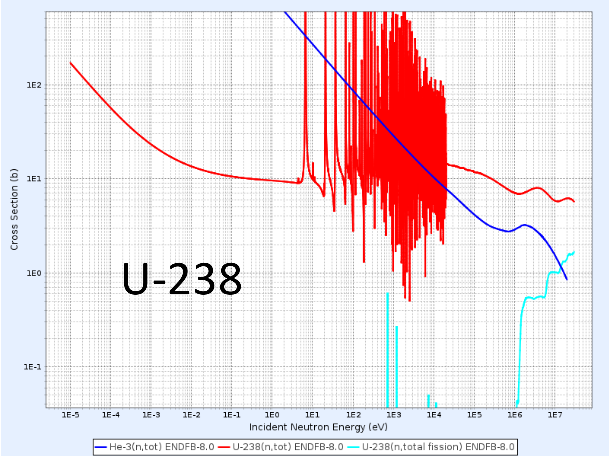

Wender et al., Nucl. Instr. Meth. A (1993) **336** 226-231

U-238/235: Fission Chamber

- LANSCE fission chamber has several different layers (U-235, U-238, blank)
  ⇒ Utilize different cross-sections
- 16” fission chamber under construction
  ⇒ fission chambers can handle large area

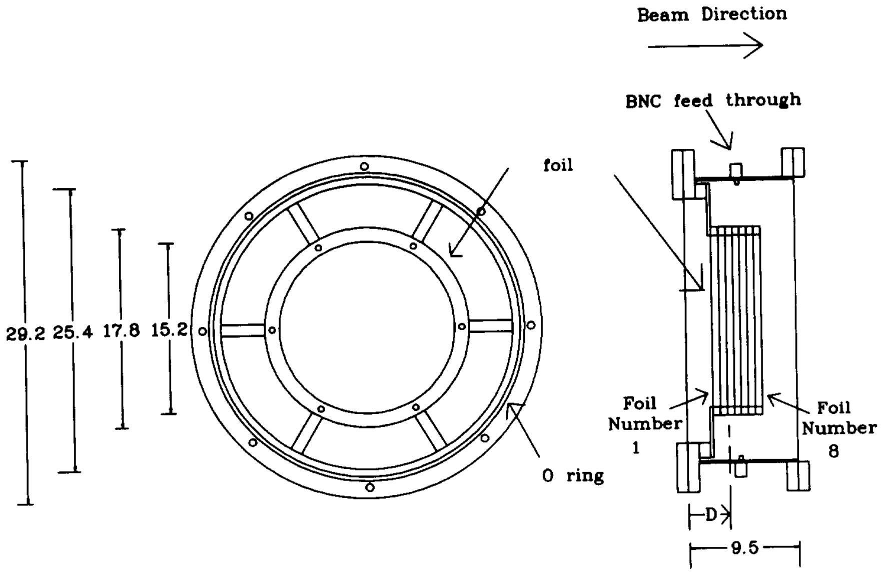

Fig. 1. Schematic diagram of the ionization chamber housing. Dimensions are in centimeters.

Table 1
Description and location of foils in chamber

Foil number	Distance D [cm]	Function
1	2.15	Ground plane
2	2.72	Deposit #1 (typically ^{235}U)
3	2.26	Signal #1
4	3.99	Deposit #2 (typically ^{238}U)
5	4.63	Signal #2
6	5.26	Deposit #3 (typically blank)
7	5 90	Signal #3
8	6 53	Ground plane

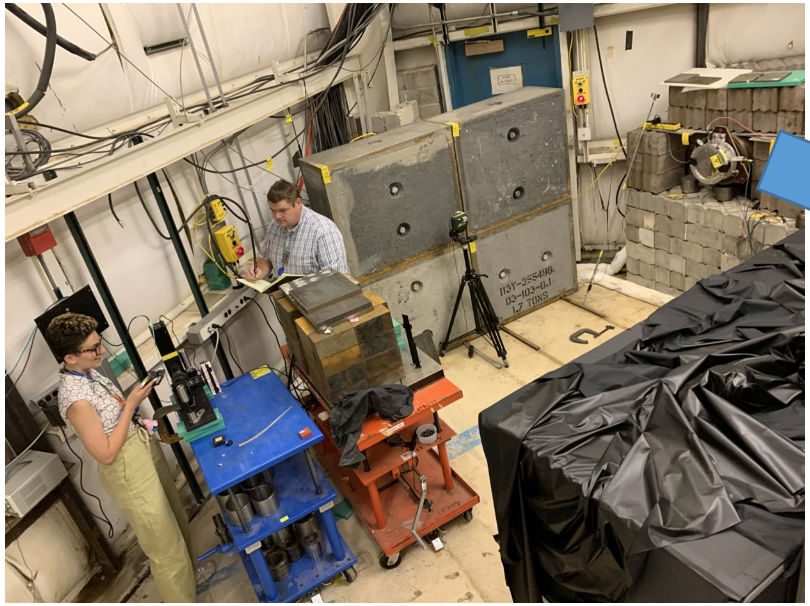

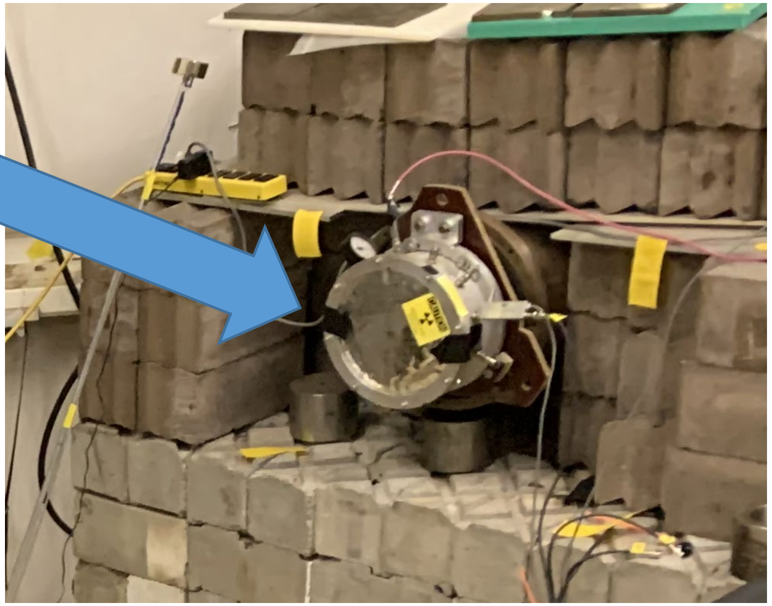

Wender et al., Nucl. Instr. Meth. A (1993) **336** 226-231

U-238/235: Fission Chamber

- LANSCE fission chamber has several different layers (U-235, U-238, blank)
  ⇒ Utilize different cross-sections
- 16” fission chamber under construction
  ⇒ fission chambers can handle large area

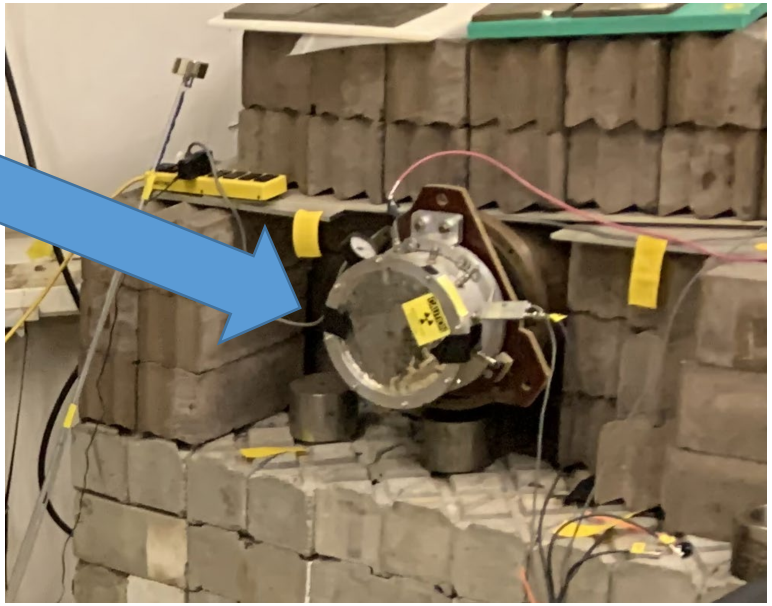

Wender et al., Nucl. Instr. Meth. A (1993) **336** 226-231

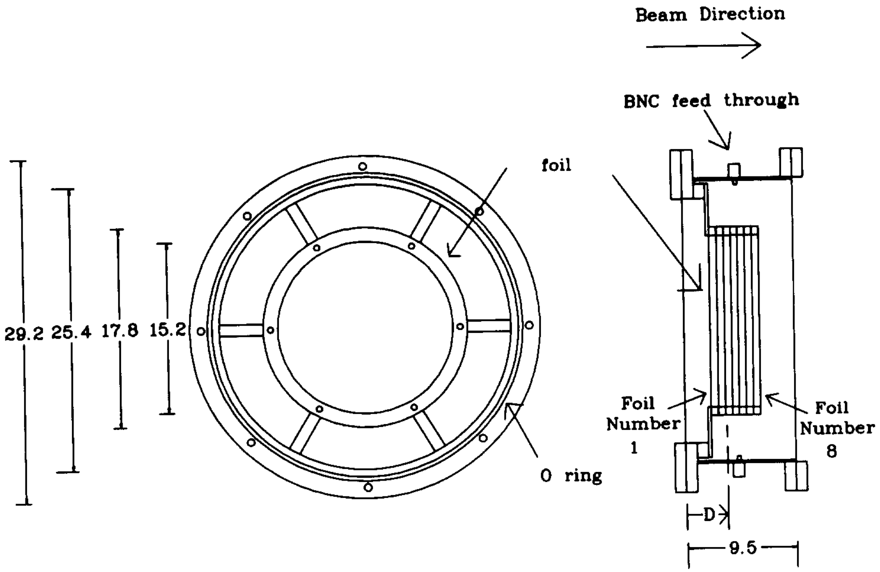

Fig. 1. Schematic diagram of the ionization chamber housing. Dimensions are in centimeters.

Table 1
Description and location of foils in chamber

Foil number	Distance D [cm]	Function
1	2.15	Ground plane
2	2.72	Deposit #1 (typically ^{235}U)
3	2.26	Signal #1
4	3.99	Deposit #2 (typically ^{238}U)
5	4.63	Signal #2
6	5.26	Deposit #3 (typically blank)
7	5 90	Signal #3
8	6 53	Ground plane

Neutron Radiography with MeV neutrons: Nanoguide scintillators

- Why neutron radiography with MeV neutrons?
- Demonstration from ~2015 by James Hunter, Ron Nelson et al. at 60R beamline
- Example: Hollow dU cylinder (15.24cm OD, 4 cm wall thickness, 20.3cm tall, 62kg $\Rightarrow$hard with X-rays…)
- “Nothing says LANL like a Nambe green chili, a Kokopelli cork and two pyrite crystals imaged in a uranium cylinder” (Ron Nelson)
- 60R has been used to characterize MeV neutron scintillators produced by Sandia, TriTEC/PSI, LANL etc.

Photograph

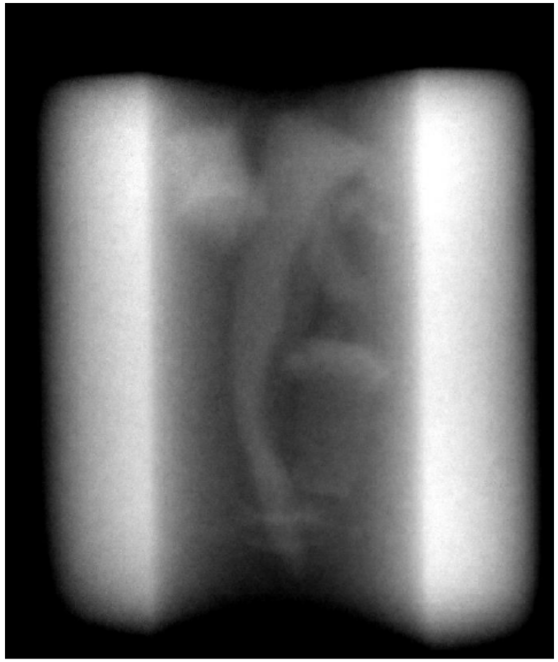

New Mexico parts with cylinder subtracted

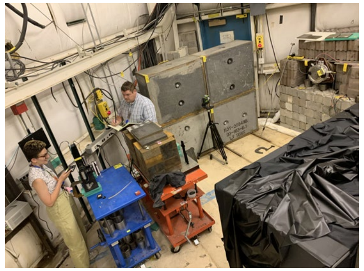

CT slice of NM parts

Courtesy J. Hunter, M. Espy, C. Gautier, R. Nelson

Neutron Radiography with MeV neutrons: Nanoguides

- Scintillators turn MeV neutrons into light
- Light can be detected
- If light is proportional to neutron intensity, we can perform MeV neutron radiography
- Interaction probability of MeV neutrons with most materials is low $\Rightarrow$ **thick scintillator for efficiency**
- Light (photons) must get out $\Rightarrow$ optically transparent
- Light created by proton recoil emitted in all directions
  $\Rightarrow$ spatial and temporal resolution lost when thick scintillator is viewed downstream
  $\Rightarrow$ **thin scintillator for spatial resolution**

Neutron Radiography with MeV neutrons: Nanoguides

- MeV neutrons destroy cameras ⇒ mirror and shielding needed
- Resolution targets ⇒ compare e.g. line-spread function
- Fission chamber ⇒ compare light output

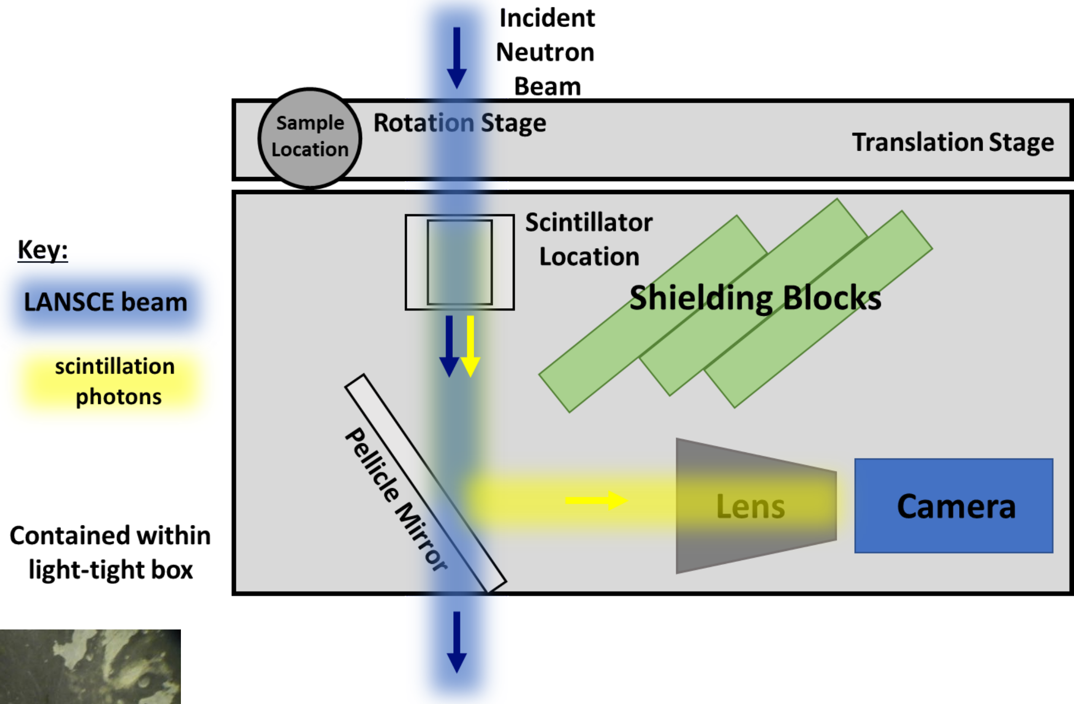

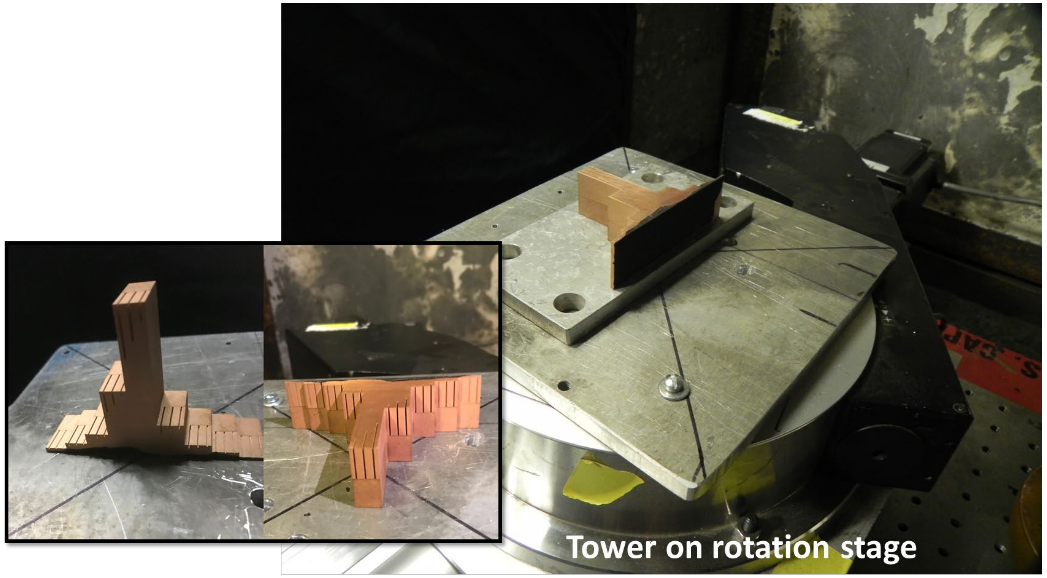
Tower on rotation stage

Neutron Radiography with MeV neutrons: Nanoguides

2021 Imaging Setup

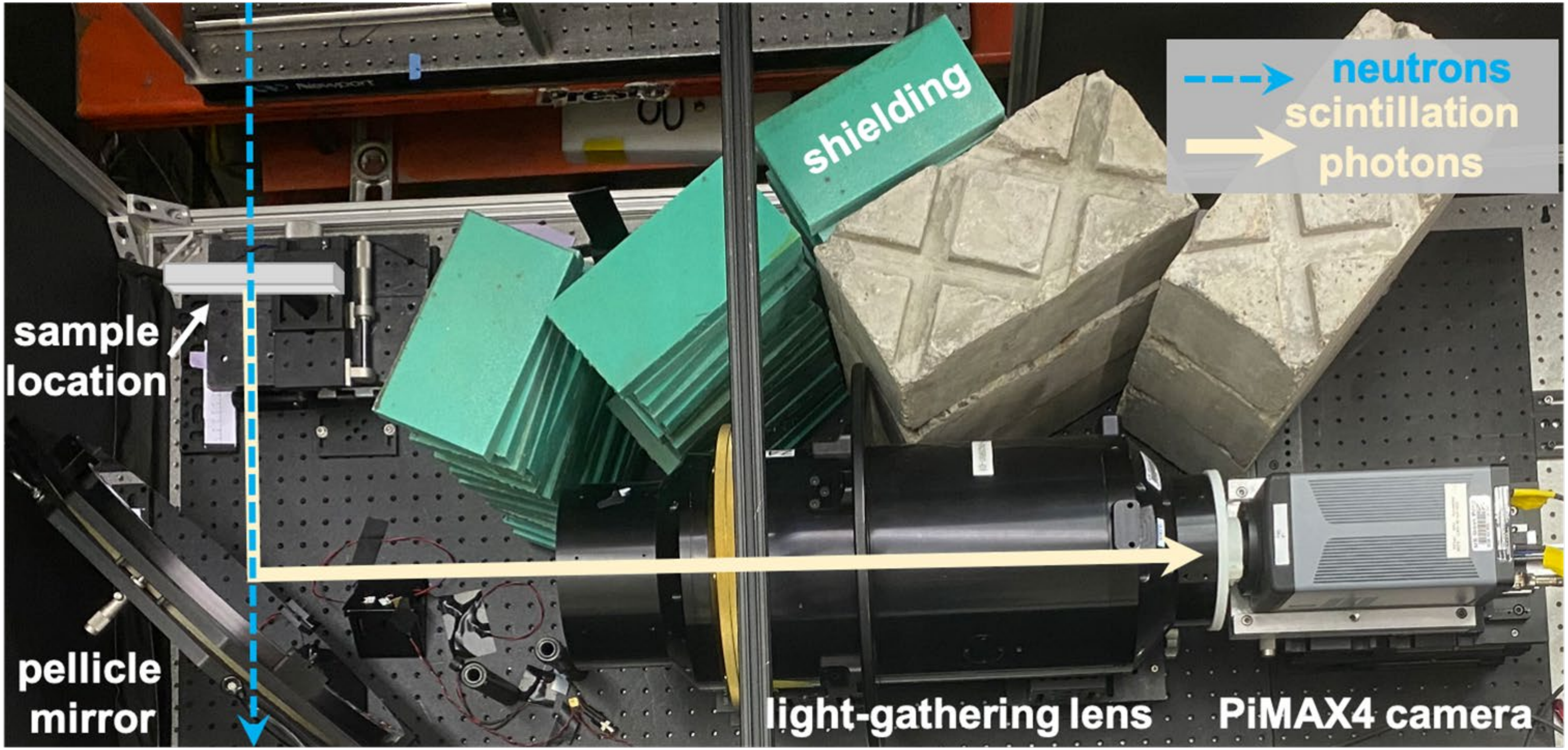

Neutron Radiography with MeV neutrons: Nanoguides

- Oftentimes there is a tradeoff between the resolution and light output of a scintillator: $\Rightarrow$ Thicker scintillator = more neutron scattering events at the cost of spatial resolution due to light spread
- ‘Nanoguide’ scintillators developed at Sandia-Livermore consist of bundles of organic scintillator glass threads (think fiber optics)
- Goal is to increase scintillator thickness without compromising resolution by guiding the scintillation light down these nanoscale domains!

‘Nanoguide’ Structure

(nanoscale domain sizes)

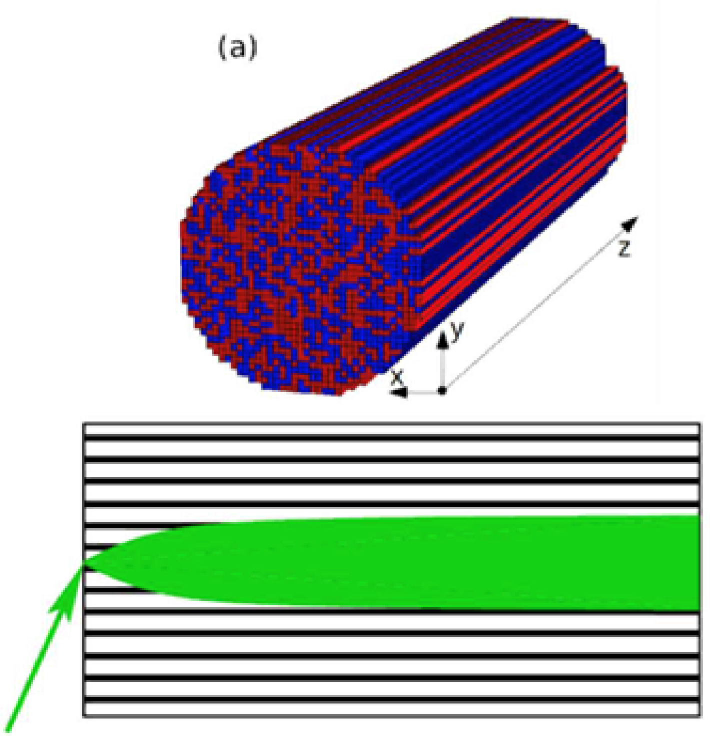

1 September 2021

Nano-segmented optical fibers containing molecular organic glass scintillator for fast neutron imaging

Nicholas R. Myllenbeck, Neil McIntyre, Alexander M. Long, Danielle Schaper, Donald C. Gautier, Sven C. Vogel, David Welker, Annabelle I. Benin, Christopher L. Reed, Patrick L. Feng

Author Affiliations +

Proceedings Volume 11838, Hard X-Ray, Gamma-Ray, and Neutron Detector Physics XXIII; 118380R (2021)
https://doi.org/10.1117/12.2596532
Event: SPIE Optical Engineering + Applications, 2021, San Diego, California, United States

Neutron Radiography with MeV neutrons: Nanoguides

- Trick is to use organic glasses and draw ~100 nm diameter fiber channels
- Larger fiber diameter provide less advantage, spatial resolution is lost

Fiber-Based Image Plate

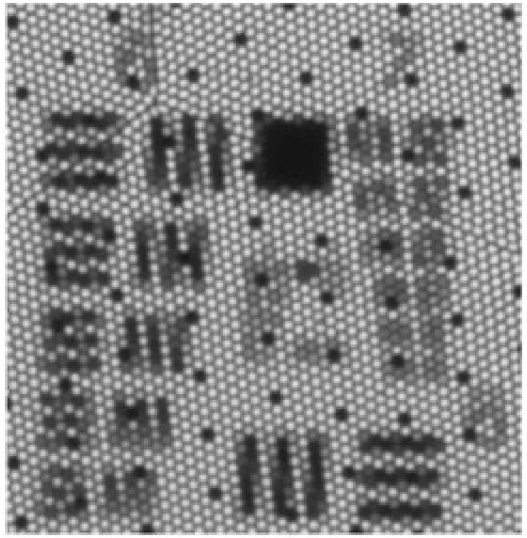

'Nanoguide' Image Plate

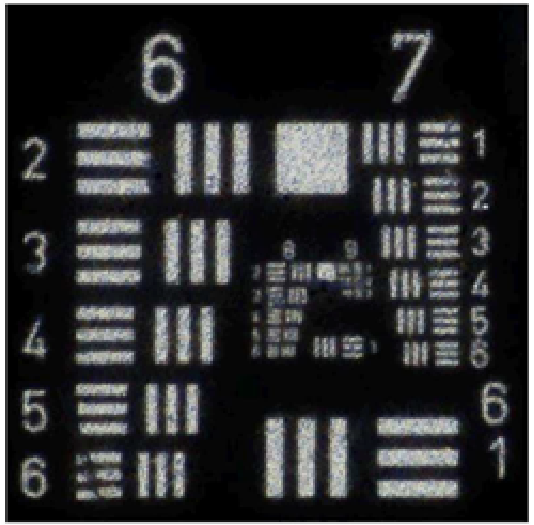

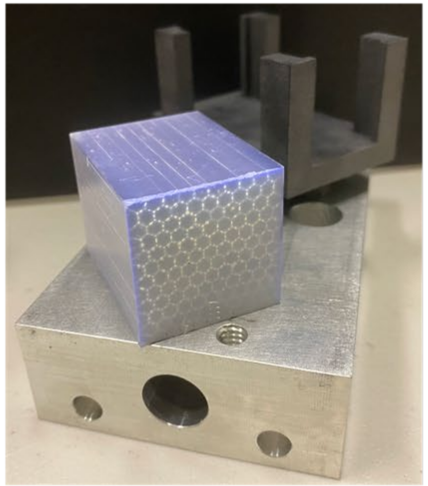

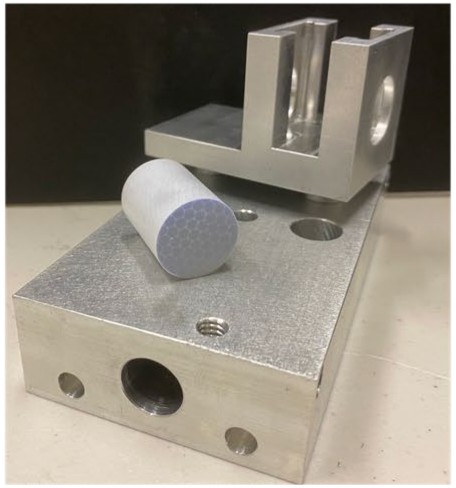

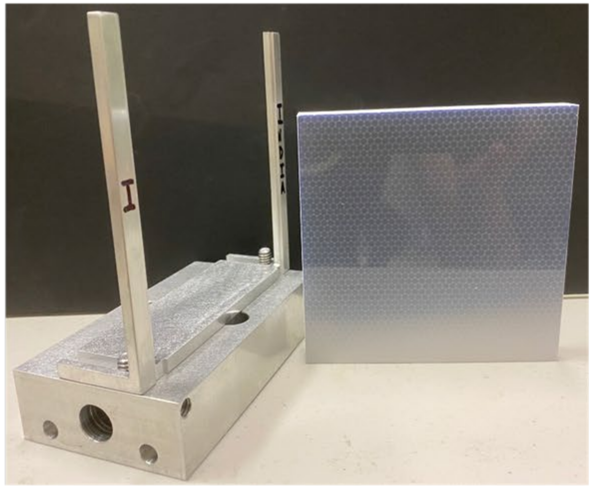

Holy grail: Pulse shape discrimination for radiography

- Event-mode cameras allow to observe individual photons with 1.6 ns time resolution within the field of view
- After identification of an event cluster originating from a single particle, pulse shape discrimination can be accomplished
  $\Rightarrow$ reject noise
  $\Rightarrow$ reject gammas
- Allows also spatial and temporal event centroiding
  $\Rightarrow$ better time-of-flight resolution
  $\Rightarrow$ better spatial resolution

Losko et al., Scientific Reports **11** (2021) 21360

Event-mode cameras: Setup

- Event-mode camera Setup

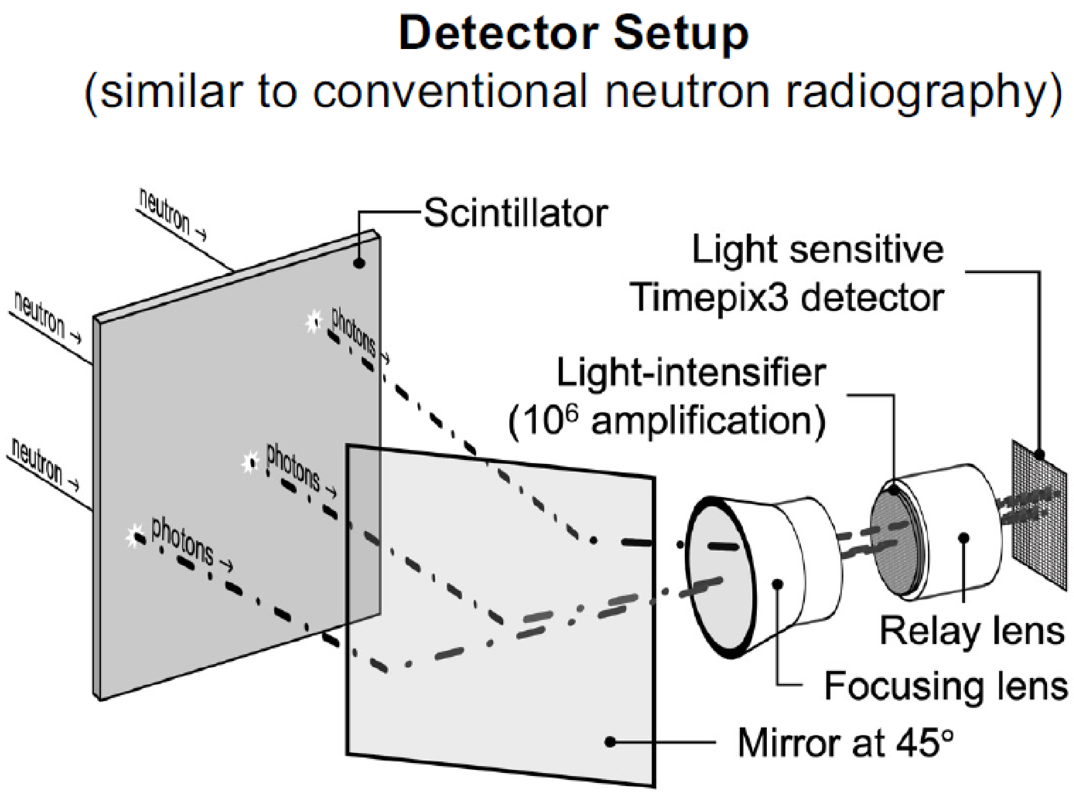

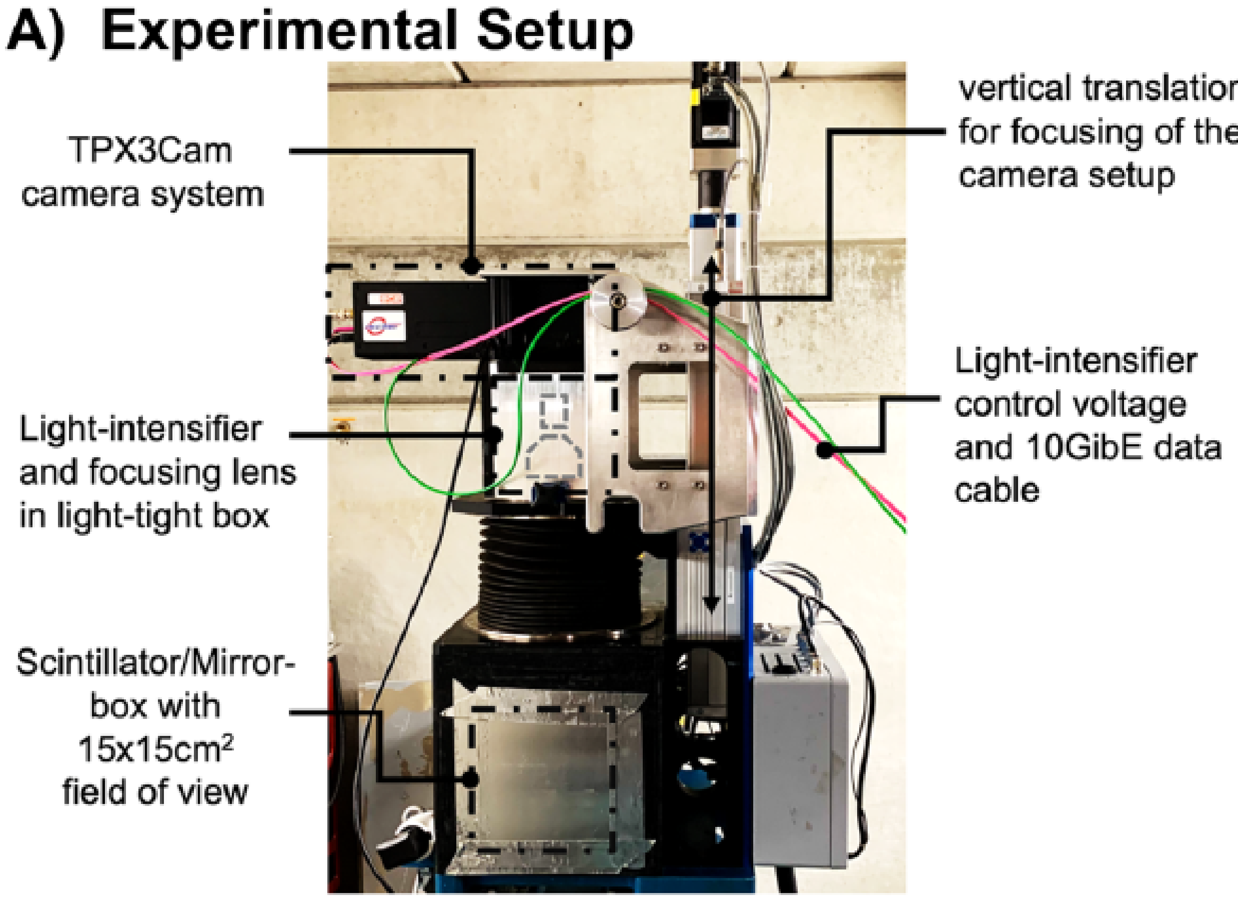

Losko et al., Scientific Reports **11** (2021) 21360

Event-mode cameras: Data processing

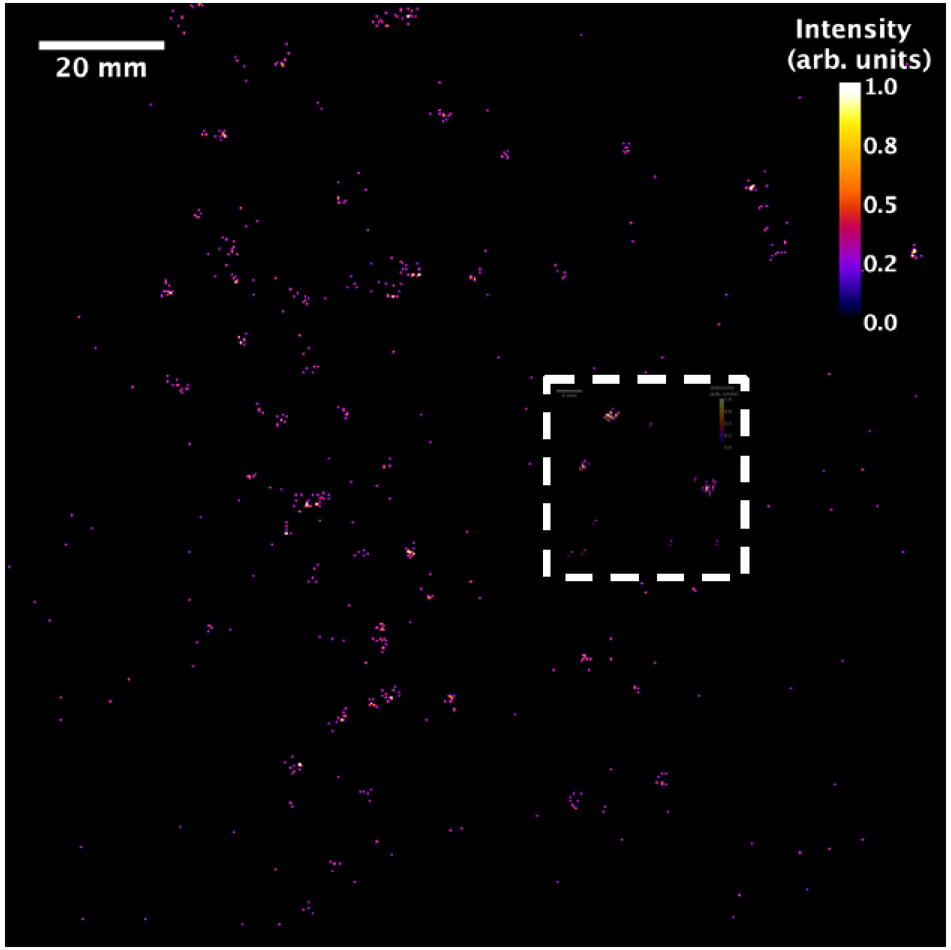

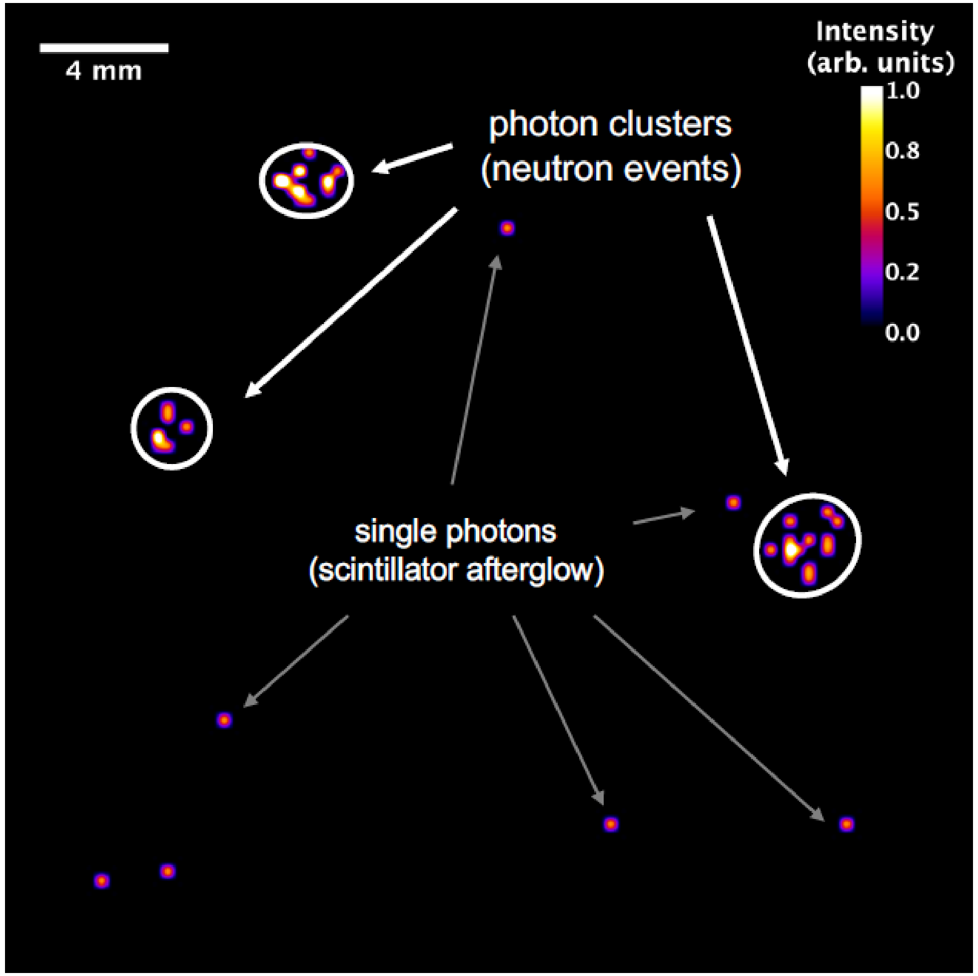

Losko et al., Scientific Reports **11** (2021) 21360

Event-mode cameras: Data processing

- Clustering provides intensity vs. time data similar to a photomultiplier tube
- BUT: In radiography mode
  $\Rightarrow$ Clean up radiography images from noise and γ
  $\Rightarrow$ Event-centroiding improves spatial and temporal resolution

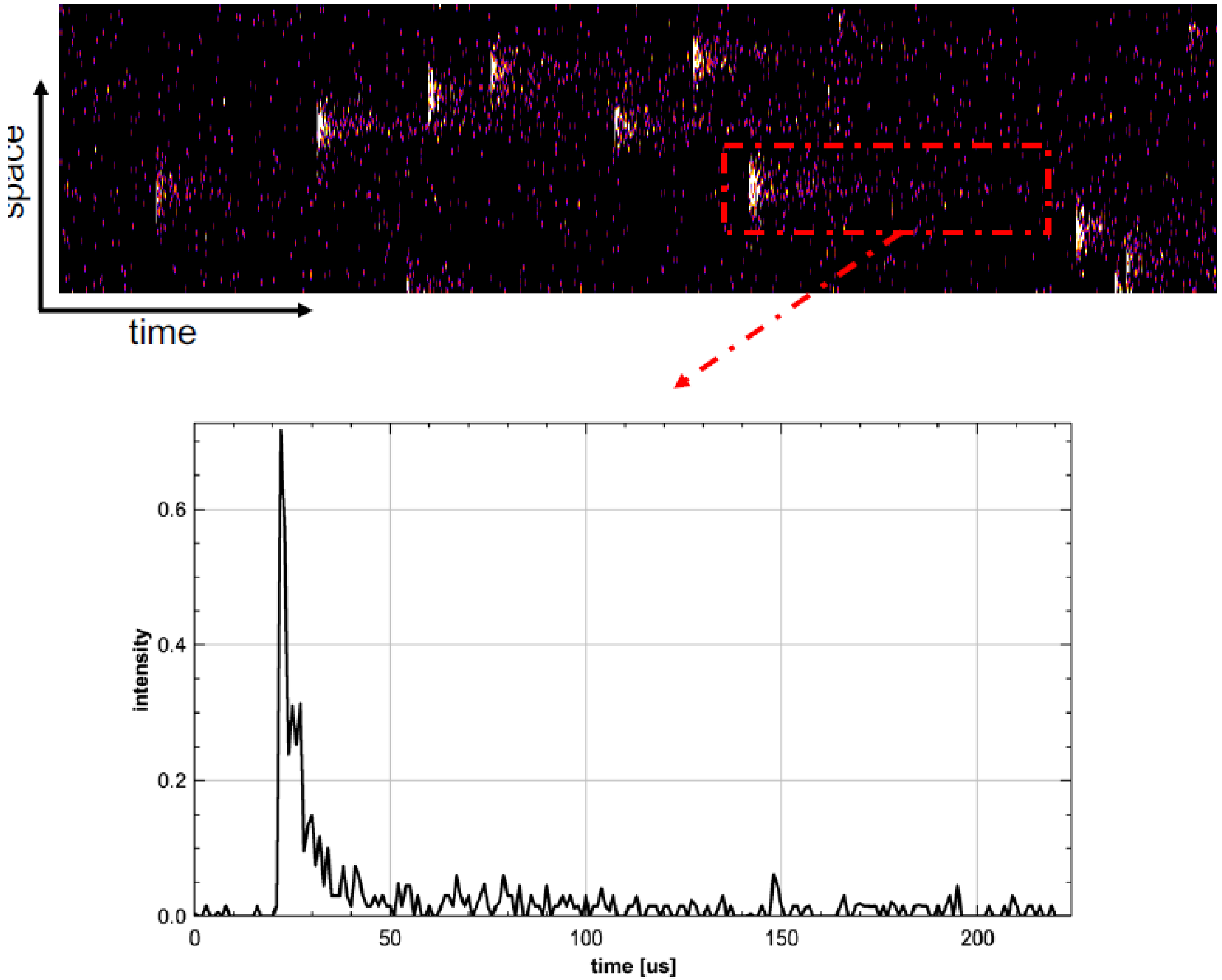

Losko et al., Scientific Reports **11** (2021) 21360

Event-mode cameras: Results

- Regular integrating radiography includes gammas, noise, no centroiding

A) Photon event mode at native detector resolution

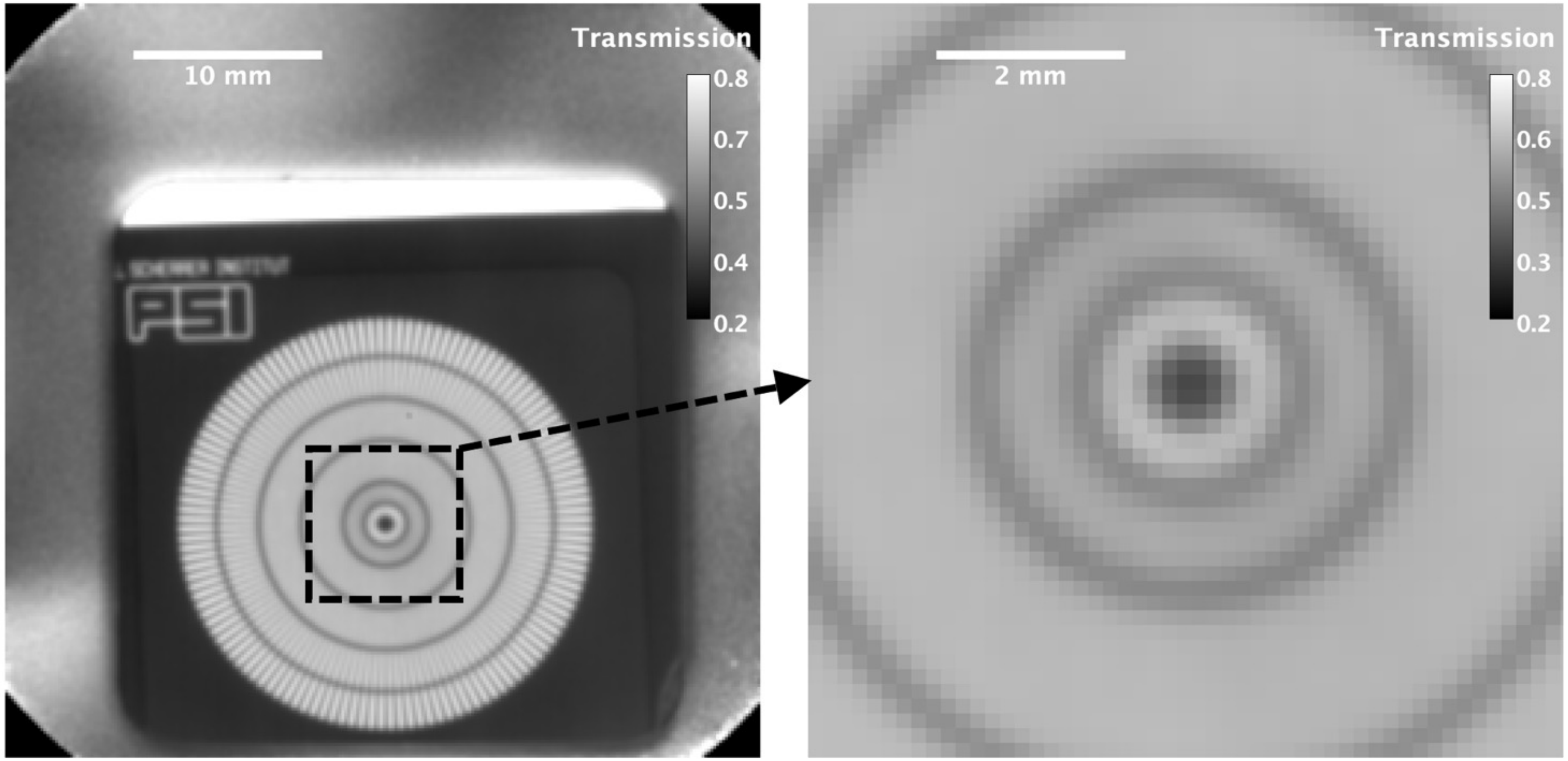

Losko et al., Scientific Reports **11** (2021) 21360

Event-mode cameras: Results

- Event-mode camera rejects gammas, noise and improves resolution by centroiding

B) Neutron event mode at super resolution

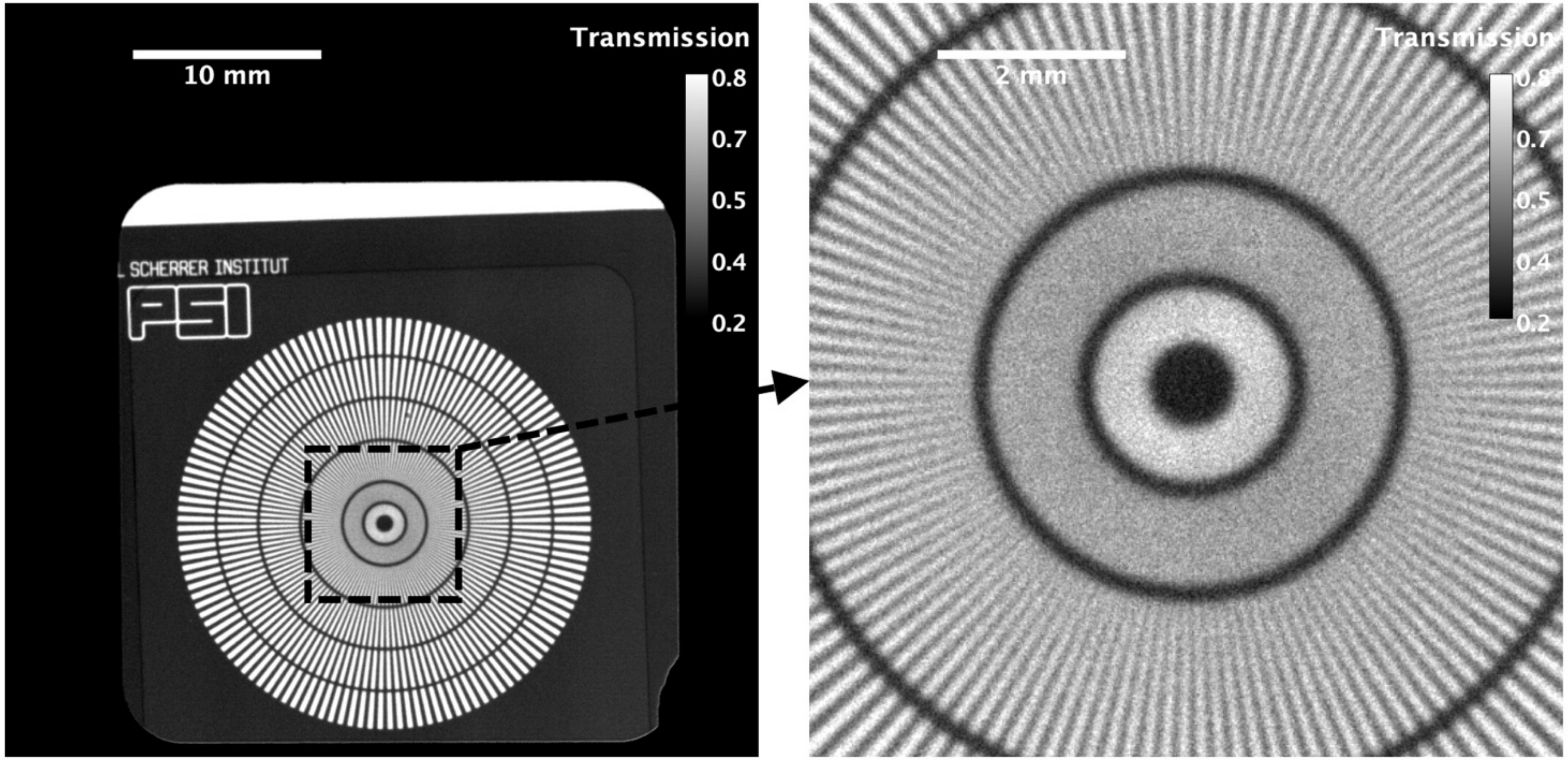

Losko et al., Scientific Reports **11** (2021) 21360

Event-mode camera: MeV resonance imaging

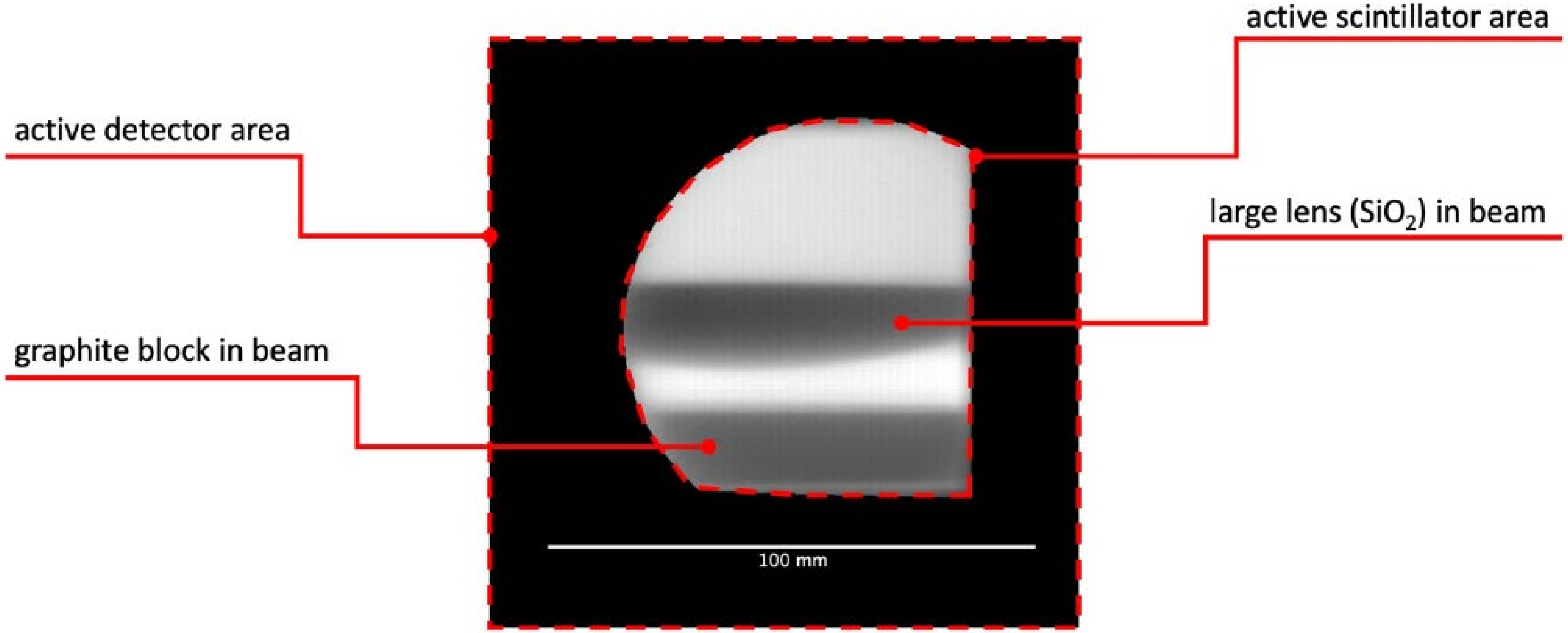

MeV neutron radiograph (30min)

Wolfertz et al., in preparation

Event-mode camera: MeV resonance imaging

- Material identification with MeV neutrons ⇒ identify light nuclei while epithermal neutrons are sensitive to heavy nuclei

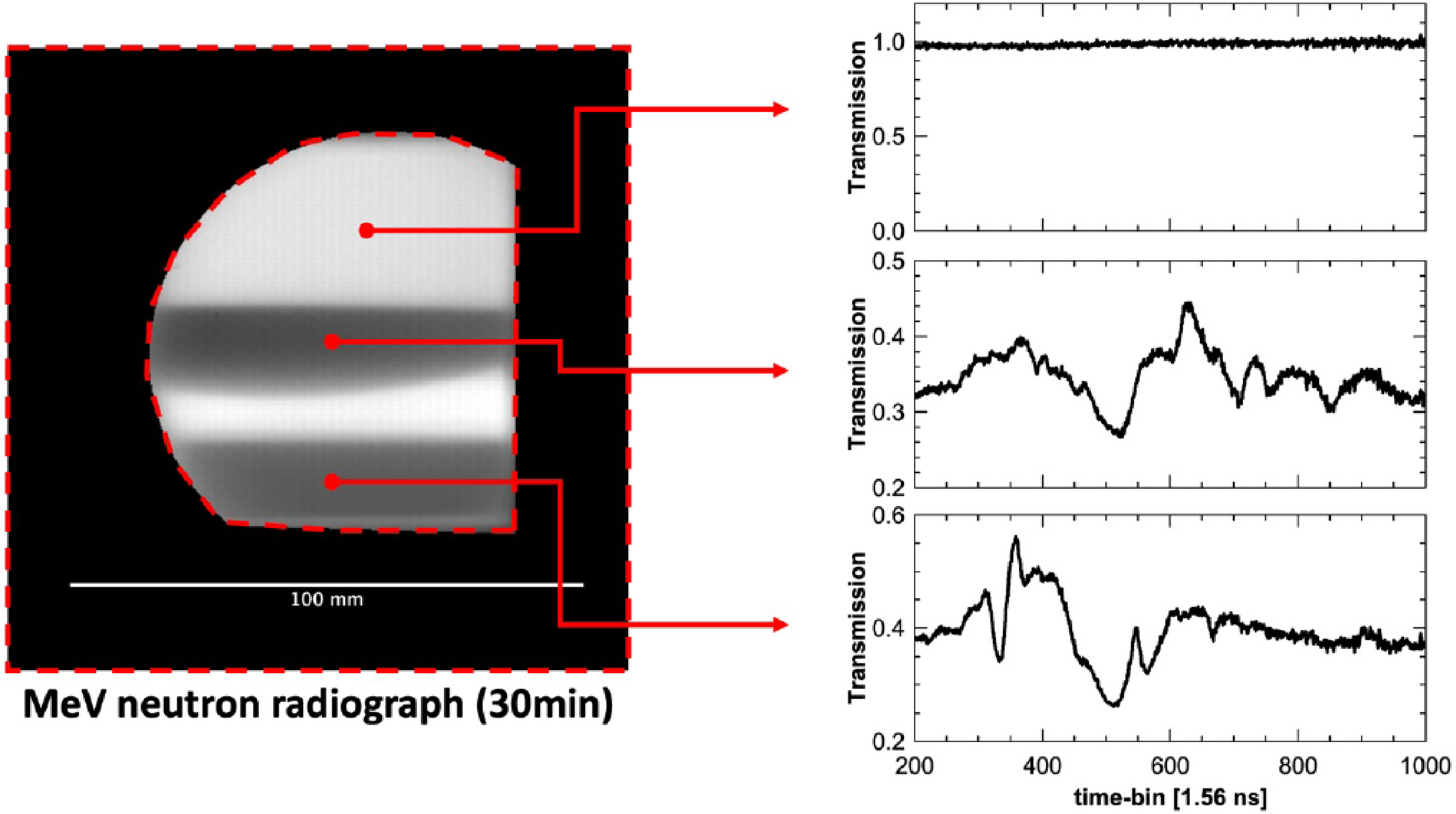

MeV neutron radiograph (30min)

Wolfertz et al., in preparation

Gold activation:
Measure absolute neutron intensity

- Gold has fairly large absorption cross-section for thermal (<0.4 eV) neutrons
- Mono-isotopic ⇒ single reaction, easy calculations
- Half-life of Au-198: ~2.7 days,
  ⇒ not too short, not too long
- Use one bare and one cadmium wrapped foil
  ⇒ Measure both thermal (<0.4 eV) and
  epithermal (>0.4 eV) intensities
- E.g. measurements at LANSCE described in detail by Ino et al. Nucl. Instr. Meth. A. **525** (2004) 496

79-Au

Available Isotopes

Au-168	Au-169 (150#us)	Au-170 (290us)
Au-171 (22.3us)	Au-172 (28ms)	Au-173 (25.5ms)
Au-174 (139ms)	Au-175 (200ms)	Au-176 (1.05s)
Au-177 (1.501s)	Au-178 (3.4s)	Au-179 (7.1s)
Au-180 (7.9s)	Au-181 (13.7s)	Au-182 (15.5s)
Au-183 (42.8s)	Au-184 (20.6s)	Au-185 (4.25m)
Au-186 (10.7m)	Au-187 (8.3m)	Au-188 (8.84m)
Au-189 (28.7m)	Au-190 (42.8m)	Au-191 (3.18h)
Au-192 (4.94h)	Au-193 (17.65h)	Au-194 (38.02h)
Au-195 (186.01d)	Au-196 (6.165d)	Au-197 (100%)
Au-198 (2.69464d)	Au-199 (3.139d)	Au-200 (48.4m)
Au-201 (26.0m)	Au-202 (28.4s)	Au-203 (60s)
Au-204 (38.3s)	Au-205 (32.0s)	Au-206 (47s)
Au-207 (3#s)	Au-208 (20#s)	Au-209 (1#s)
Au-210 (10#s)		

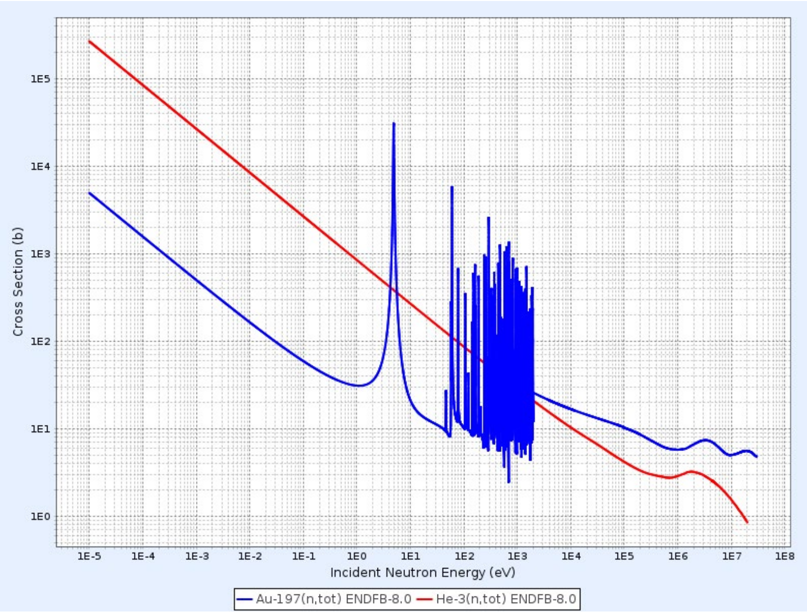

Silver activation: Pulsed neutron beam monitors

- Far West Technology, Inc. model 2080
  ⇒ standard monitor at LANSCE
- 9” polyethylene sphere moderates neutrons
- Two Geiger-Muller counters, one wrapped in silver foil, one in foil of tin
- Silver: Ag-107 and Ag-109 have substantial absorption cross-section for thermal neutrons
- Half-lives of activation products are ~2:25 minutes and 0:25 minutes
  ⇒ reasonably fast for real time alarms

47-Ag

Available Isotopes

Ag-92 (1#ms)	Ag-93 (228ns)	Ag-94 (27ms)
Ag-95 (1.78s)	Ag-96 (4.45s)	Ag-97 (25.5s)
Ag-98 (47.5s)	Ag-99 (2.07m)	Ag-100 (2.01m)
Ag-101 (11.1m)	Ag-102 (12.9m)	Ag-103 (65.7m)
Ag-104 (69.2m)	Ag-105 (41.29d)	Ag-106 (23.96m)
Ag-107 (51.839%)	Ag-108 (2.382m)	Ag-109 (48.161%)
Ag-110 (24.56s)	Ag-111 (7.433d)	Ag-112 (3.130h)
Ag-113 (5.37h)	Ag-114 (4.6s)	Ag-115 (20.0m)
Ag-116 (3.83m)	Ag-117 (73.6s)	Ag-118 (3.76s)
Ag-119 (6.0s)	Ag-120 (1.52s)	Ag-121 (777ms)
Ag-122 (529ms)	Ag-123 (294ms)	Ag-124 (177.9ms)
Ag-125 (160ms)	Ag-126 (52ms)	Ag-127 (89ms)
Ag-128 (60ms)	Ag-129 (49.9ms)	Ag-130 (40.6ms)
Ag-131 (35ms)	Ag-132 (30ms)	Ag-133

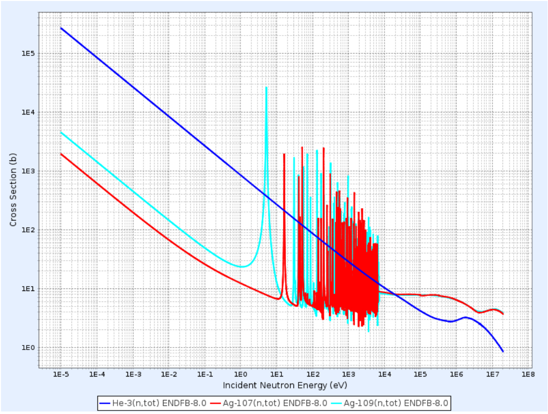

Bubble chambers

- Passive neutron dosemeter (no real time read out)
- Developed by Bubble Technology Industries,
- Bubbles form through induced nucleation of super-heated droplets
- Bubbles are counted and converted to neutron dose
- Re-heat bubble chamber for re-use
- Insensitive to gammas
- Response to neutrons fairly flat from 0.3 to 35 MeV
- Robust, no setup needed
  $\Rightarrow$ Often first tests if neutrons were produced

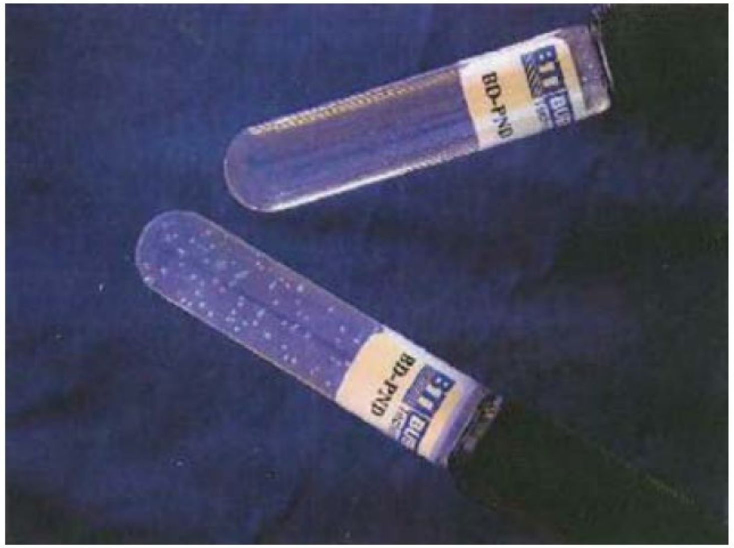

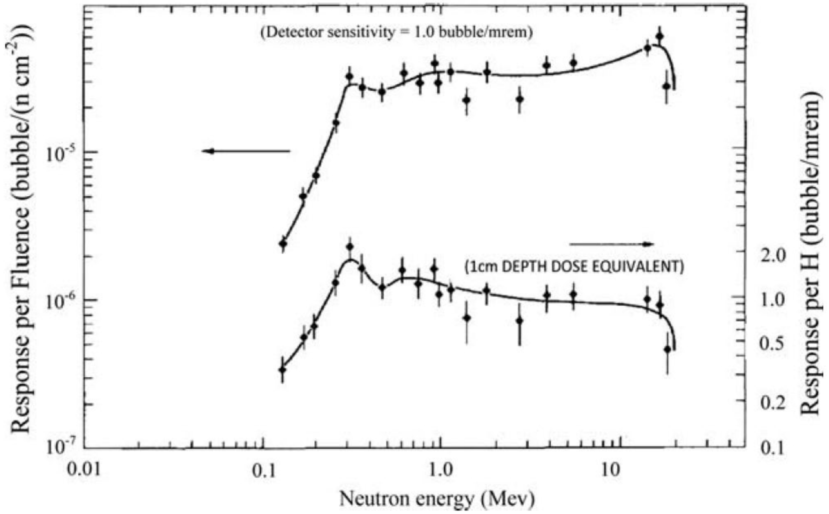

Figure 3. BD-PND normalised response per unit fluence (closed circles) and response per unit dose equivalent (closed diamonds). Conversion from fluence to dose equivalent based on NCRP Report No. 38[17].

Lewis et al., Radiation Protection Dosimetry **150** (2012) 1–21

Recent results from Fort Collins with bubble chambers

- 25J laser pulses at up to 3.3 Hz (burst mode, short time) or 1 Hz or less for hours
- Limiting factor for laser repetition rate is cooling of optics
- Goal of the beam time: Explore X-ray source size smaller than conventional X-ray sources for radiography applications
- X-rays produced by sending laser pulses on 1 to 3 mm thick tungsten disks $\Rightarrow$ Bremsstrahlung
- Uneven surface of tungsten disks (micrometers) requires pre-scan to adjust laser focus to maximize yield
- Home-made motion control (alignment, rotation etc.)
- Some Bremsstrahlung X-rays are high enough in energy to produce photo-neutrons
- Tungsten happens to be one of the best materials for that to happen $\Rightarrow$ decent neutron source
- Brought Tremsin neutron detectors from LANSCE to characterize LDNS at Fort Collins

Setup at Colorado State University

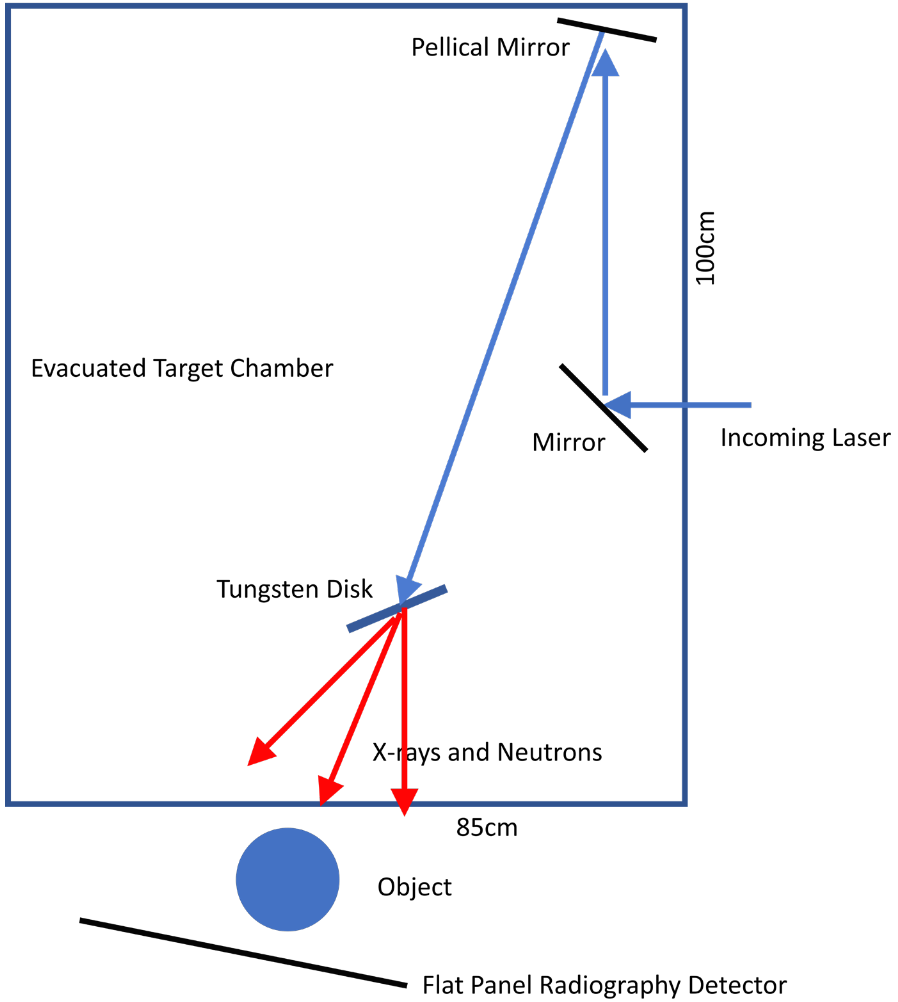

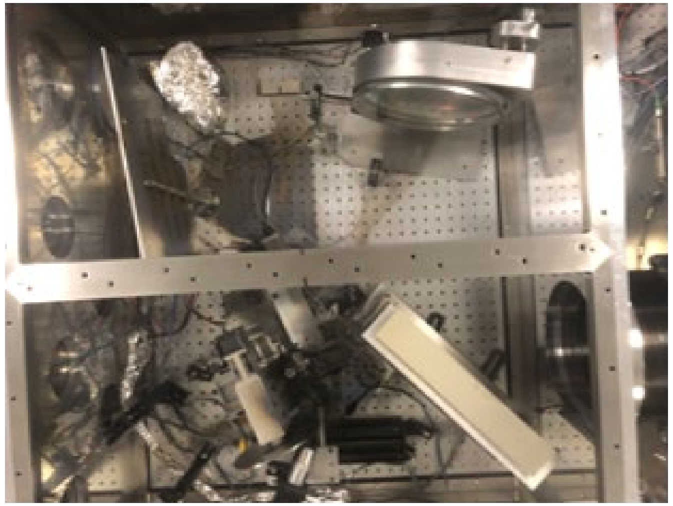

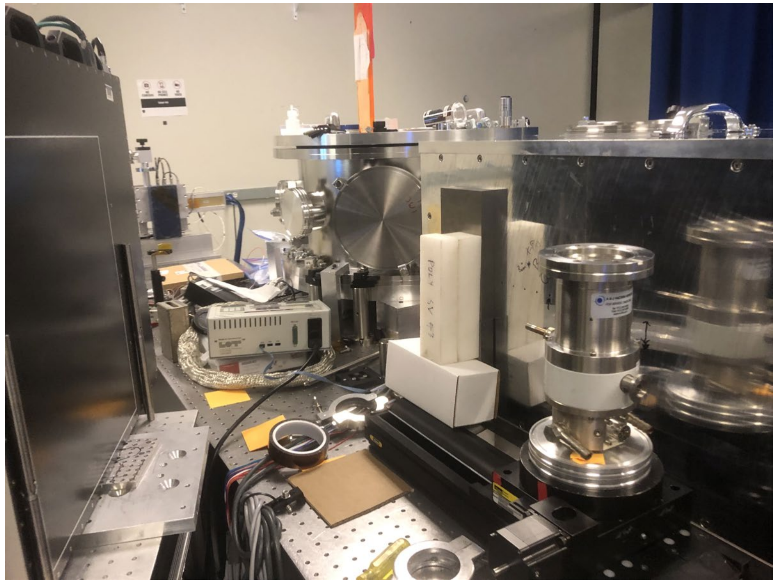

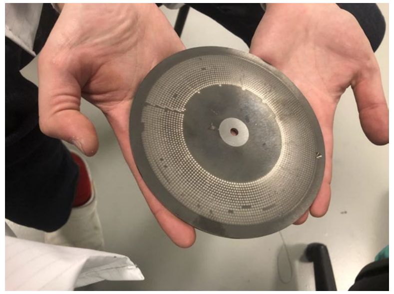

X-ray radiography & tomography

- X-ray CT reconstruction of turbo pump
- ~1000 single shots
- Small source size provides great magnification
- Short pulse length provide negligible motion blur for blades spinning at 40,000 rpm (pump was not spinning during the CT)
- MeV energies provide penetration through metal

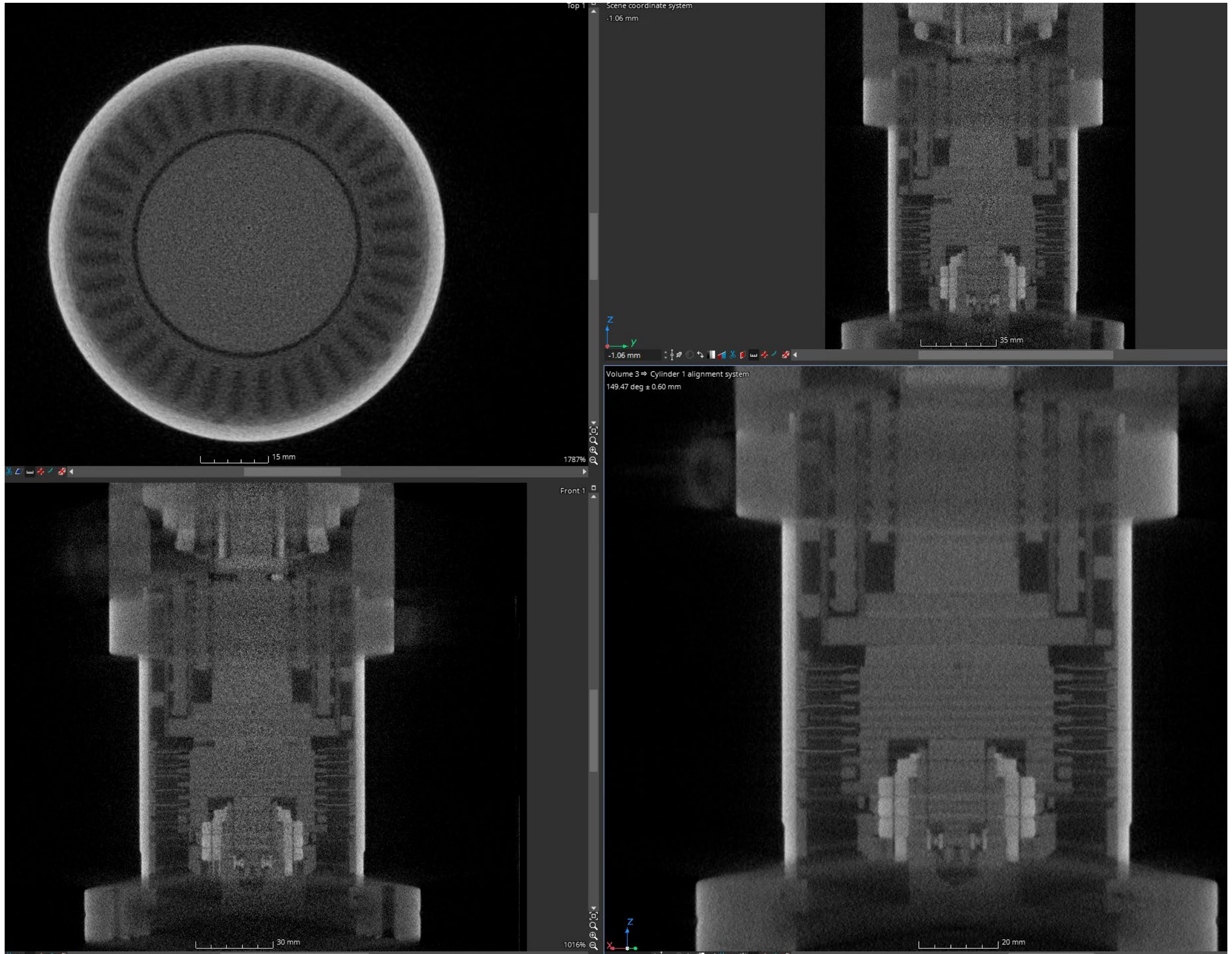

Bubble Chamber Characterization

- Bubble chambers ~uniform sensitivity for neutrons between 0.3 and 35 MeV $\Rightarrow$ neutrons as produced, not thermal neutrons
- Number of bubbles proportional to dose
- Dose ~proportional to number of neutrons (correct conversion factor is important!)
- Normalize by solid angle (distance, chamber dimensions)

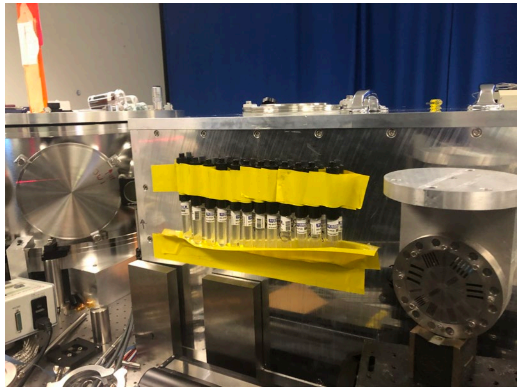


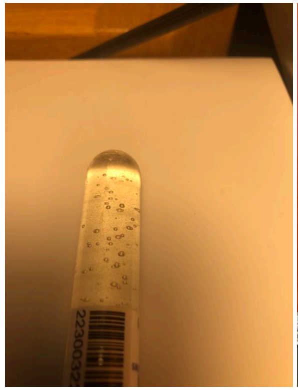


Bubble Chambers Results #1

Bubbles after 10 laser pulses on 3mm W disk

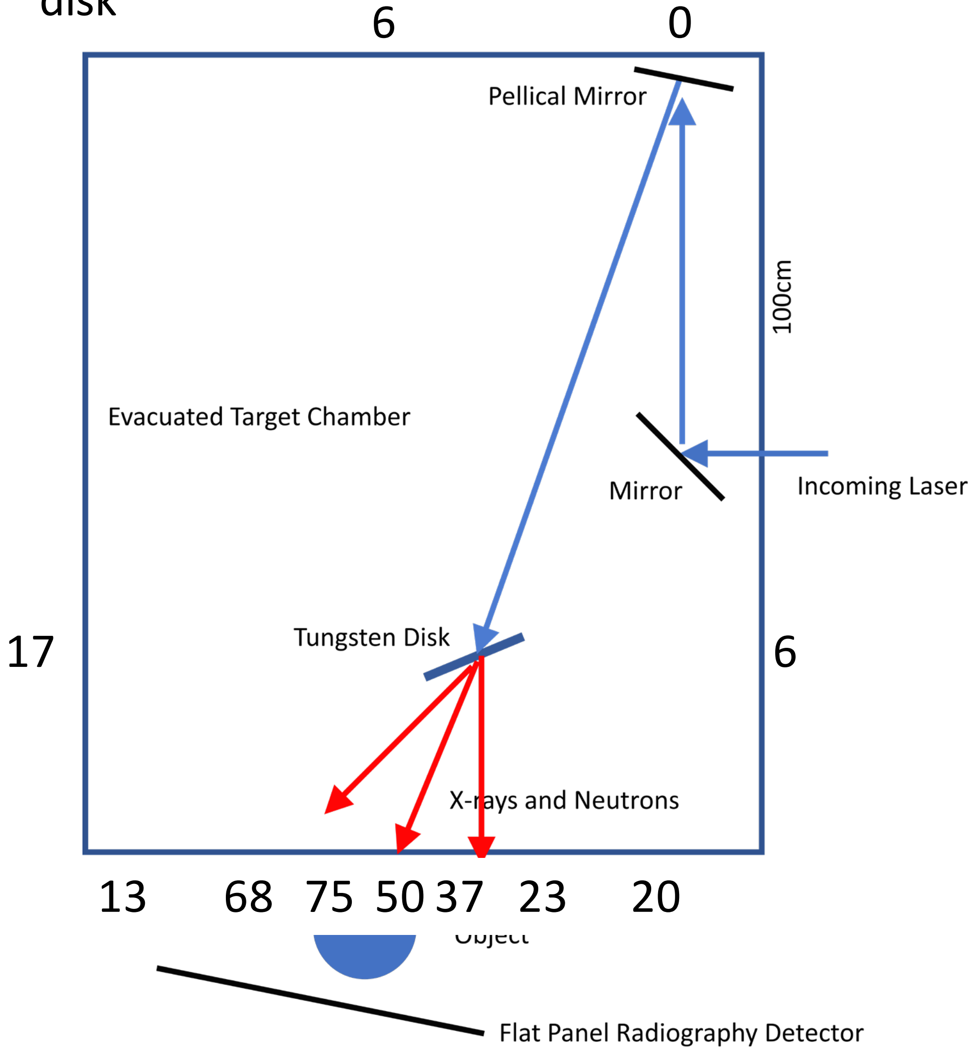

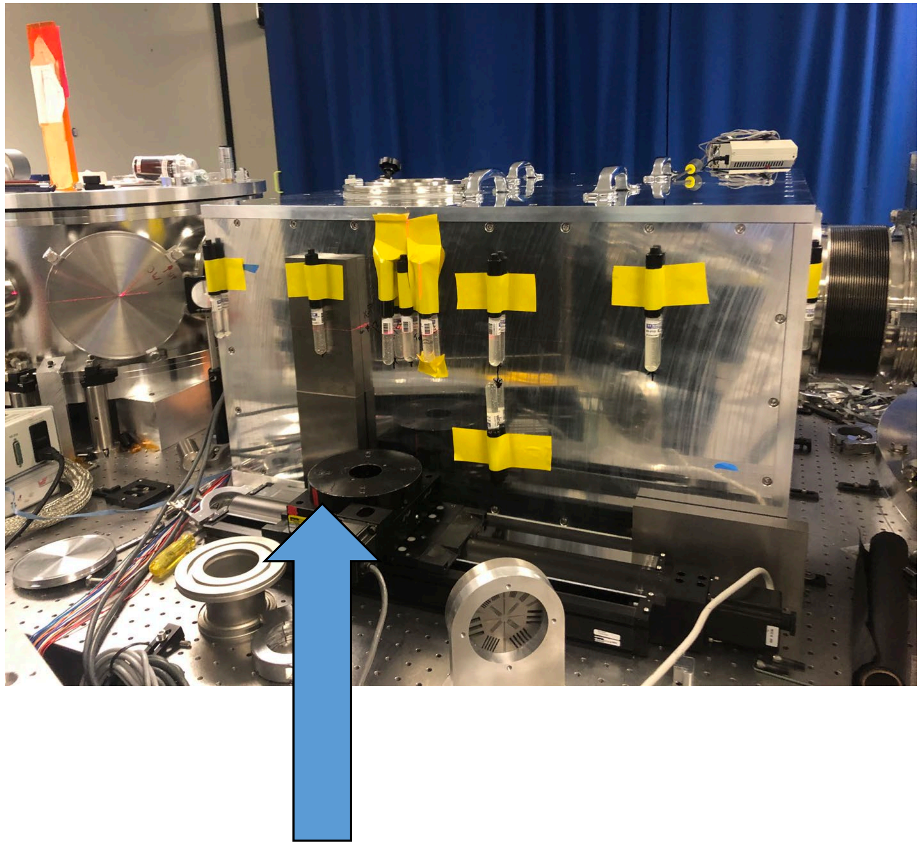

1” thick tungsten to shield X-ray radiography flat panel
⇒ secondary target?

Bubble Chambers Results #2

- 1mm tungsten target produces ~twice as many neutrons as 2mm and 3mm
- Off-center shift observed (no W block)
- Total number consistent with ~1 million neutrons per pulse

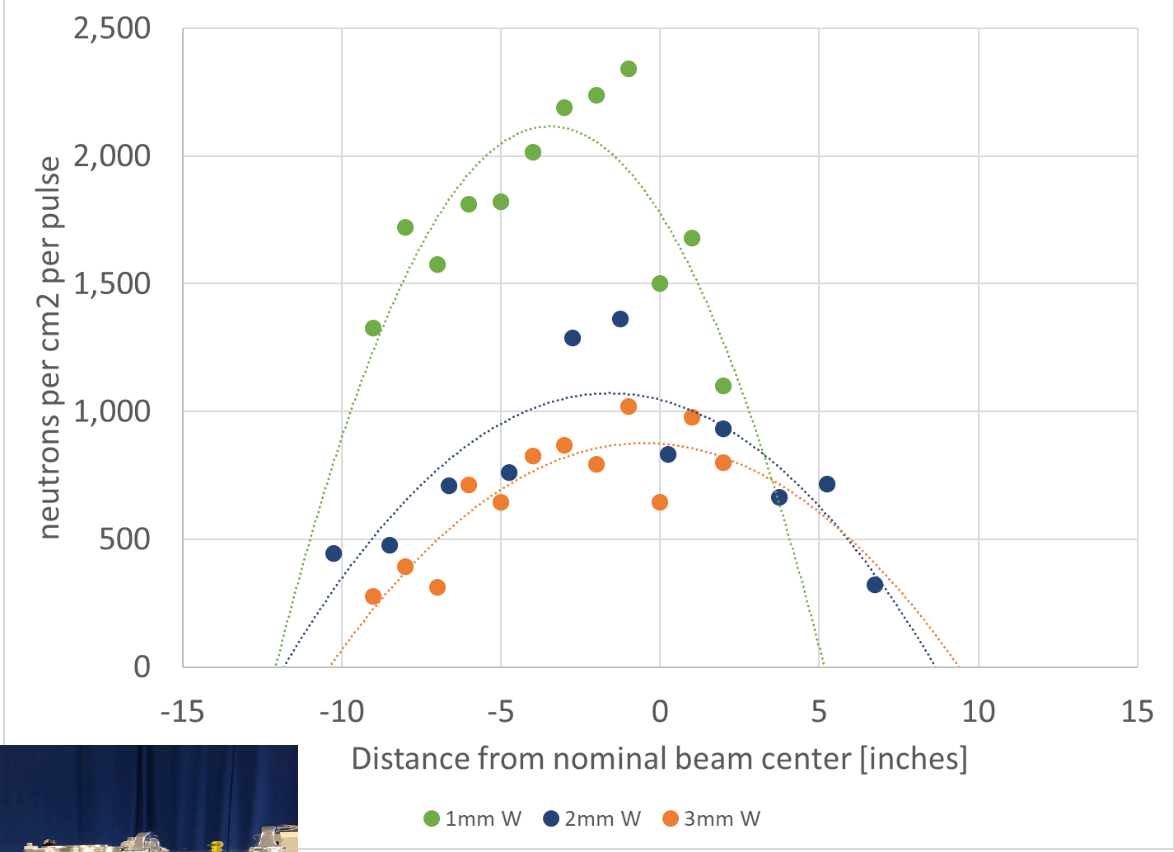

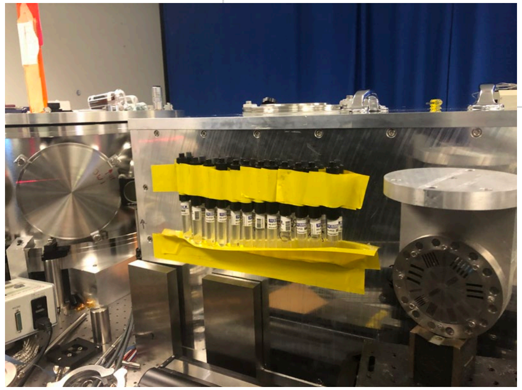

THE END

Thank you for your attention!

sven@lanl.gov